Integrated Flood Risk Analysis and Management Methodologies

FLOODsite

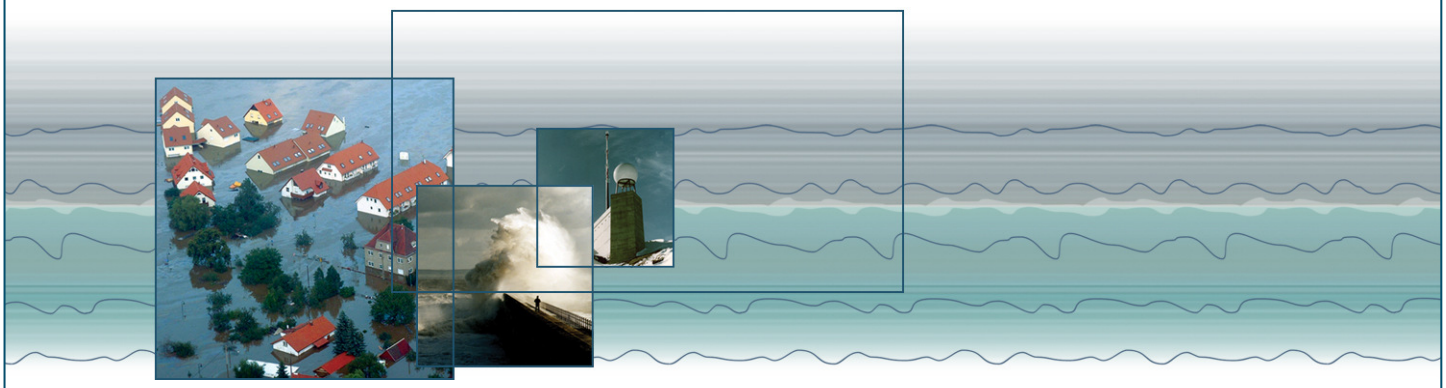

Laboratory Tests on the Erosion of Clay Revetment of Sea Dike With and Without a Grass Cover Induced by Breaking Wave Impact

LWI REPORT NR 935

Date **May 2007**

Report Number **T04-07-11**
Revision Number 1_0_P03

Task Leader Partner

FLOODsite is co-funded by the European Community
Sixth Framework Programme for European Research and Technological Development (2002-2006)
FLOODsite is an Integrated Project in the Global Change and Eco-systems Sub-Priority
Start date March 2004, duration 5 Years

Document Dissemination Level

PU	**Public**
PP	Restricted to other programme participants (including the Commission Services)
RE	Restricted to a group specified by the consortium (including the Commission Services)
CO	Confidential, only for members of the consortium (including the Commission Services)

Co-ordinator: HR Wallingford, UK
Project Contract No: GOCE-CT-2004-505420
Project website: www.floodsite.net

SIXTH FRAMEWORK PROGRAMME

DOCUMENT INFORMATION

Title	**Laboratory Tests on the Erosion of Clay Revetment of Sea Dike with and without a Grass Cover Induced by Breaking Wave Impact**
Lead Author	**Grzegorz Stanczak**
Contributors	**Hocine Oumeraci, Andreas Kortenhaus**
Distribution	**Task 4 and 6 Partners**
Document Reference	**[**Click here and enter Document Reference**]**

DOCUMENT HISTORY

Date	Revision	Prepared by	Organisation	Approved by	Notes
01/06/06	1_0_P03	GS	LWI		1st Draft

ACKNOWLEDGEMENT

The work described in this publication was supported by the European Community's Sixth Framework Programme through the grant to the budget of the Integrated Project FLOODsite, Contract GOCE-CT-2004-505420.

DISCLAIMER

SUMMARY

This report addresses the preparation and performance of laboratory tests on a the erodibility of clay cover with and without grass, subjected to impact pressures generated by controlled falling water mass

Three types of clay, representing different erosion resistances as well as grass cover of moderate quality have been used in order to gain information on the processes of surface erosion and shear failure within a crack in a dike cover subject to impact pressures. A computer-controlled system was applied to generate the impact pressures in the range 12-25 kPa by using a mass of water which is suddenly dropped from a given height.

The conceptual model of Führböter (1966) on the shear failure of a crack in a clay revetment is compared to the experimental results. The shear failure itself did indeed occur. However, the failure mechanism significantly differs from the predicted one. The tests with the clay samples subject to a series of impact pressure events provided results that fit relatively well with the model of Torri et al. (1987). The coefficients describing the parameters of the soil and the damping effect of the water layer were calibrated using the experiments.

A new empirical approach to calculate the influence of the root network on the erosion of grass due to impact pressures and contribution to existing theories are discussed. The results are expected to considerably contribute to a better understanding of the mechanisms and to the prediction of breach initiation of sea dikes.

NOTATIONS AND SYMBOLS

a	-	Depth of the crack [m]
A	-	Area of the sides of a soil block [m^2]
b	-	Parameter describing the influence of the roots on the erodibility of the soil [-]
B_n	-	N-th classification factor according to Weißmann (2003) [-]
c	-	Cohesion [Pa]
c_r	-	Apparent root cohesion [Pa]
d	-	Depth under the surface of the soil [cm]
d_{crit}	-	Critical erosion depth [cm]
D	-	Parameter describing the quality of the grass cover [-]
E_k	-	Kinetic energy of the impact [J]
F_{crack}	-	Force acting on the wall of a crack [N]
g	-	Acceleration due to gravity [m/s^2]
G	-	Mass of a soil block [N]
h	-	Water layer thickness [cm]
h_f	-	Fall height [m]
h_w	-	Water level in pipe [m]
H_s	-	Significant wave height [m]
I_p	-	Plasticity index [-]
k_d	-	Empirical detachability parameter for clay [cm^3/J]
$k_{d,p}$	-	Empirical detachability parameter for clay [cm^3/kPa]
$k_{d,g,p}$	-	Empirical detachability parameter for grass [cm^3/kPa]
$k_{d,g,t}$	-	Empirical detachability parameter for the whole revetment [cm^3/kPa]
k_f	-	Infiltration rate [m/s]
l	-	Length of the shear failure plane [m]
L	-	Length of the crack [m]
m_R	-	Mass of roots [kg]
N	-	Classification number according to Weißmann (2003) [-]
p_{max}	-	Maximum impact pressure acting on the surface [Pa]
$p_{max,crit}$	-	Critical impact pressure [Pa]
Q	-	Reaction of the soil [N]
R_d	-	Volume of soil eroded for a single impact pressure event (in general) [cm^3]
$R_{d,g,p}$	-	Volume of soil eroded for a single impact pressure event - grass [cm^3]
$R_{d,p}$	-	Volume of soil eroded for a single impact pressure event - clay [cm^3]
$R_{d,t,p}$	-	Volume of the soil eroded for a single impact pressure event - whole cover [cm^3]
RVR	-	Root volume ratio [%]
S	-	Shear force [N]
S_p	-	Sand percentage [%]
$t_{30\%}$	-	Decomposition time [s]
T_r	-	Root tensile strength [Pa]
U	-	Pore water pressure [Pa]
V_R	-	Volume of roots [m^3]
V_s	-	Shrinkage [%]
V_{ss}	-	Volume of a single sample of grass cover [m^3]
w	-	Parameter characterizing the damping effect of a water layer [-]
w_c	-	Water content [-]
w_l	-	Flow limit [-]
W	-	Shear strength [N]
α	-	Angle of shear failure [^{0}]
α_{calc}	-	Calculated angle of shear failure [^{0}]
α_{meas}	-	Measured angle of shear failure [^{0}]
ρ_R	-	Density of dry grass roots [kg/m^3]
Δt	-	Time of impact pressure [s]
φ	-	Angle of internal friction [^{0}]

ρ	-	Density of the water [kg/m^3]
ρ_R	-	Density of dry grass roots [kg/m^3]
θ	-	Root angle of shear rotation [^{0}]
τ	-	Shear strength of the soil [Pa]

CONTENTS

Tables

Figures

1. Introduction

Low-lying coastal areas in Germany as well as in other countries such as in The Netherlands and Denmark are protected from flooding by sea dikes. Breaches of those structures are regarded as the main cause of flood disasters. A dike breach usually occurs due to high water levels during a storm surge and repeated action of waves. The breach may be initiated either from the land side by wave overtopping and overflow or from the seaside by breaking wave impact on the dike slope.

A failure of a dike from the seaside can be initiated as a result of

- impact pressures acting on a water-filled cracks or
- due to surface erosion of the grass and clay cover

Existing conceptual models on the processes taking place within a crack subject to impact pressures (Führböter, 1966) have never been verified in laboratory experiments. The approaches to calculate the surface erosion (Woolhiser et al, 1990) have yet been verified only for a limited range of impact pressures and only for clay cover.

In order to develop a reliable prediction model for the dike breaching initiated from the seaside by the breaking wave impact, it is necessary to investigate experimentally the related processes that lead to the breach initiation and consequently to the breaching of a sea dike.

This report addresses the preparation, performance and analysis of laboratory tests on a clay cover with and without grass, subjected to impact pressures generated by a controlled falling water mass. The report is structured as follows:

Chapter 2 describes briefly the clay used as a material for dike revetments, its geotechnical properties and available models allowing one to calculate the possible failure.

In Chapter 3 the main objectives of the laboratory experiments are formulated, the experimental set-up is presented and the testing programme for the clay with and without grass is described.

Chapter 4 provides the information on the experimental results, their comparison with theoretical predictions and suggested improvements to the existing conceptual models.

2. Clay as a dike cover

Sea-dike is a manmade earthen structure consisting of a sand core that is protected from the effects of wave action by a clay cover, with or without vegetation. The clay layer is usually about 0.8-1.5m thick, the depth of roots penetration varies between 0.1 and 0.4m depending on the grass quality and season of the year - in winter the rooting depth decreases significantly in comparison to the value measured in summer. A cross-section of a typical sea-dike built on the coast of the German North Sea is shown in Fig.1.

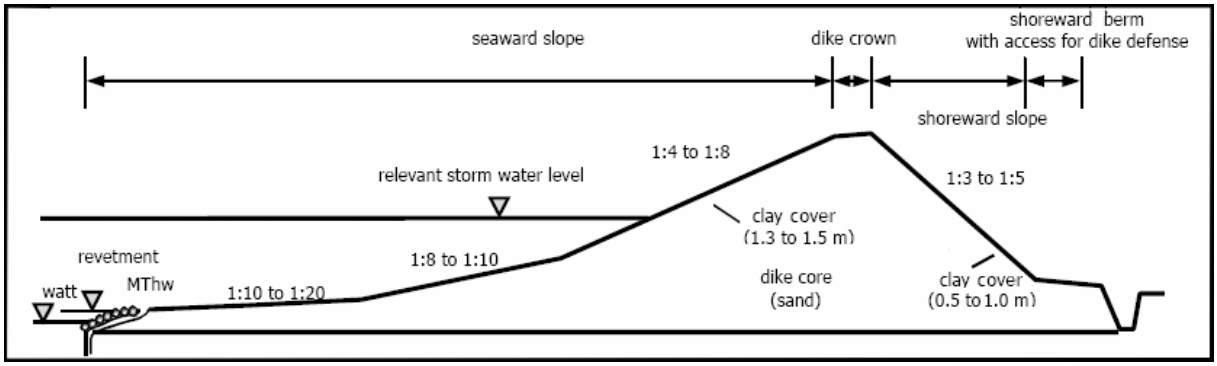

Figure 1: Cross-section of a typical dike on the German North Sea

The clay in a sea dike cover is subjected to changes in water content that may occur due to drying and wetting of a dike. Differences in suction pressure result in changes in the water content that leads to changes of the clay volume, the order of magnitude of those changes is of about half the change in water content (expressed in mass percentage). As a result, clay shrinks and expands and those processes in the unsaturated zone lead to the formation of two types of cracks (TAW,1996):

• pull-cracks usually occur when soil shrinks. These cracks are differently oriented according to their size - larger shrinkage cracks are almost always vertical while smaller cracks may occur in all directions;
• shear cracks usually occur in shear areas that are caused by the swelling of clay. Those cracks may occur in all directions.

Crack formation produces a soil that consists of aggregates of various dimensions. The composition of the cracks and aggregates, together with pores and aggregates made by burrowing animals, is called the "**soil structure**" (TAW,1996).

The formation of "soil structure" depends both on the properties of the clay itself (interaction between soil particles and water, for instance), as well as on the external factors that determine changes in suction pressure.

The biological activity in the soil should also be mentioned as a factor that influences the development of "soil structure". Burrowing animals and grass roots are responsible for a certain dynamics of the "soil structure" - new aggregates are continually being formed and then collapse again.

The development of the "soil structure" can be more or less pronounced. The strongly developed "soil structure" occurs when soil is subjected to continuous expanding and shrinkage or in case of single but very strong shrinkage. This kind of development is characterized by the aggregates that are clearly individually recognisable and that show only few connections with each other. The second type of "soil structure" (i.e. fine one) occurs due to rapid changes in water content, e.g., due to rainfall.

In Fig.2 a cross-section of a typical sea-dike cover made of clay with vegetation is shown. Significant pull-cracks can be observed. In the uppermost decimetres under the grass sod on a dike bank the "soil structure" is usually strongly developed and consists of relatively small (i.e. millimetres to centimetres) aggregates that are often linked to each other by roots (TAW,1996). At depths greater than about 50cm under the grass cover the aggregates are often less clearly recognisable.

The presence of the "soil structure" influences the hydraulic permeability of the clay layer. The top layer of clay with clearly developed "soil structure" has a considerably greater permeability than that measured on compacted clay samples. The same effect is induced by the root penetration from vegetation growing on the dike (TAW,1996). At greater depths "soil structure" may occur as a result of worm tunnels that deeply penetrate into the dike. Consequently, the hydraulic permeability of the entire clay cover is affected. In Table 1 the hydraulic permeability values for the clay cover are given for different soil structures.

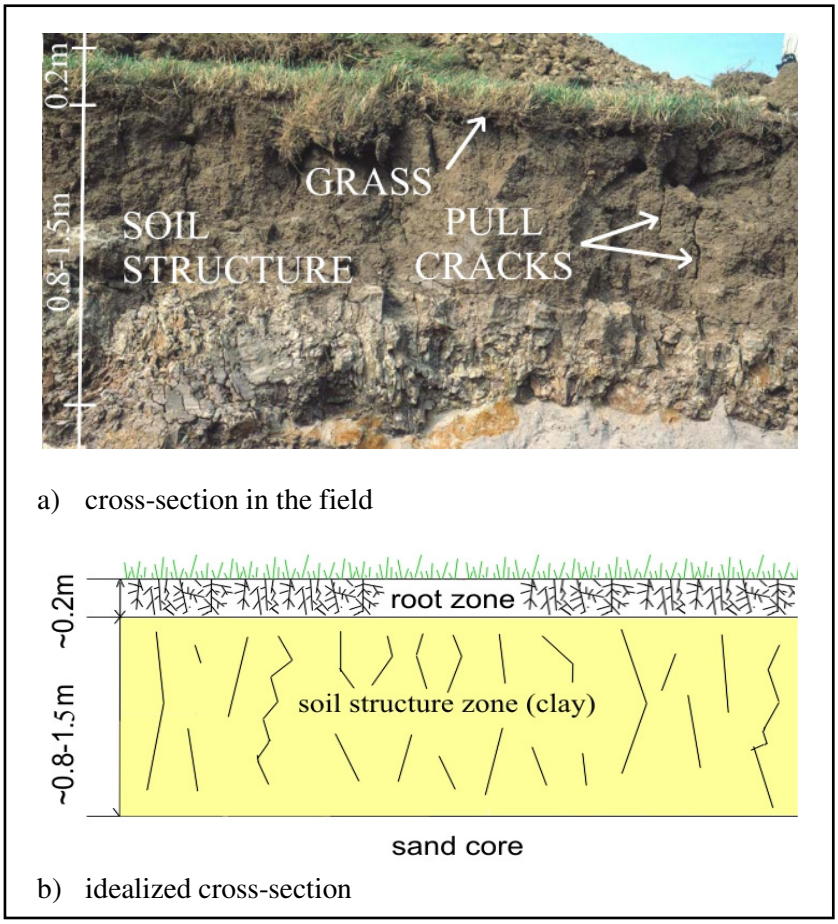

Figure 2: Clay cover of a sea dike. Soil structure and cracks are clearly recognisable (adopted from TAW,1996)

Table 1: Hydraulic permeability of clay for different conditions (order of magnitude)

Conditions of clay cover	Hydraulic permeability [m/s]
Directly after construction	10^{-6}
Fine "soil structure"	10^{-5}
Large cracks and worm tunnels	10^{-4}

The formation of the "soil structure" considerably limits the homogeneity of a clay layer as a network of coarse pores occurs. The bulk properties of a clay package with the "soil structure" differ therefore

strongly from those of individual aggregates. In a strongly structured soil, surface water infiltrates rapidly and a considerable amount of water can be drained off through the large cracks and tunnels. The soil structure formation is favourable and even essential for vegetation and other soil life, since aeration is greatly improved and roots can find an easier way into the soil (TAW,1996).

Although clay itself is regarded as an appropriate material for the dike cover, it is usually reinforced by a grass cover. The most important role in keeping the particles and small aggregates in the soil together is played by grass roots (Fig.3).The coarser roots together with small and large aggregates of soil form a dense network, while the fine root hairs keep the small particles together because they are anchored within the substrate. The dense network of roots also prevents larger pull-cracks to occur.

Figure 3: Structure of the grass roots system - principle sketch (TAW,1996)

2.1 Effects of breaking wave impact on the clay cover stability

The breaking wave impact on a dike slope may result in relatively small surfaces exposed for a very short period of time (0.01 to 0.1 s) to very high impact pressures (in the range up to 150 kPa). This impact load does not work sequentially, but intermittently in time intervals of at least one wave period (usually longer with predominant impact in the water pad, that remains after the preceding wave), so that the actual loading duration (0.1 to 0.01 s) is small in comparison with the time period between the loads (5- 12s). Therefore, it is meaningless to use the common permissible soil stress both for static and for dynamic loads as a measure for the dike load. In fact, the damage of the clay cover is caused by a variety of mechanisms that is related to:

- breaking wave impact pressures directly on the slope (represented as force A in Fig.4b) which may lead to surface erosion

- washing-out of soil particles and aggregates due to pressures acting from within the dike (force B in Fig.4b);

- effect of impact pressures acting on water-filled cracks (force E in Fig.4c);

• water movement over the dike slope following the expansion of the water jet hitting the slope (Forces C and D in Fig.4a and Fig.4b).

In the case of clay with no significant pull-cracks, usually only the surface erosion due to impact pressures and flow induced by wave run-up and run-down occurs. The available methods to calculate this type of erosion are briefly described in Section 2.1.1. The models that enable one to calculate the effects of impact pressures on larger, water-filled cracks that are often found in clay with strongly developed "soil structure" are described in Section 2.1.2

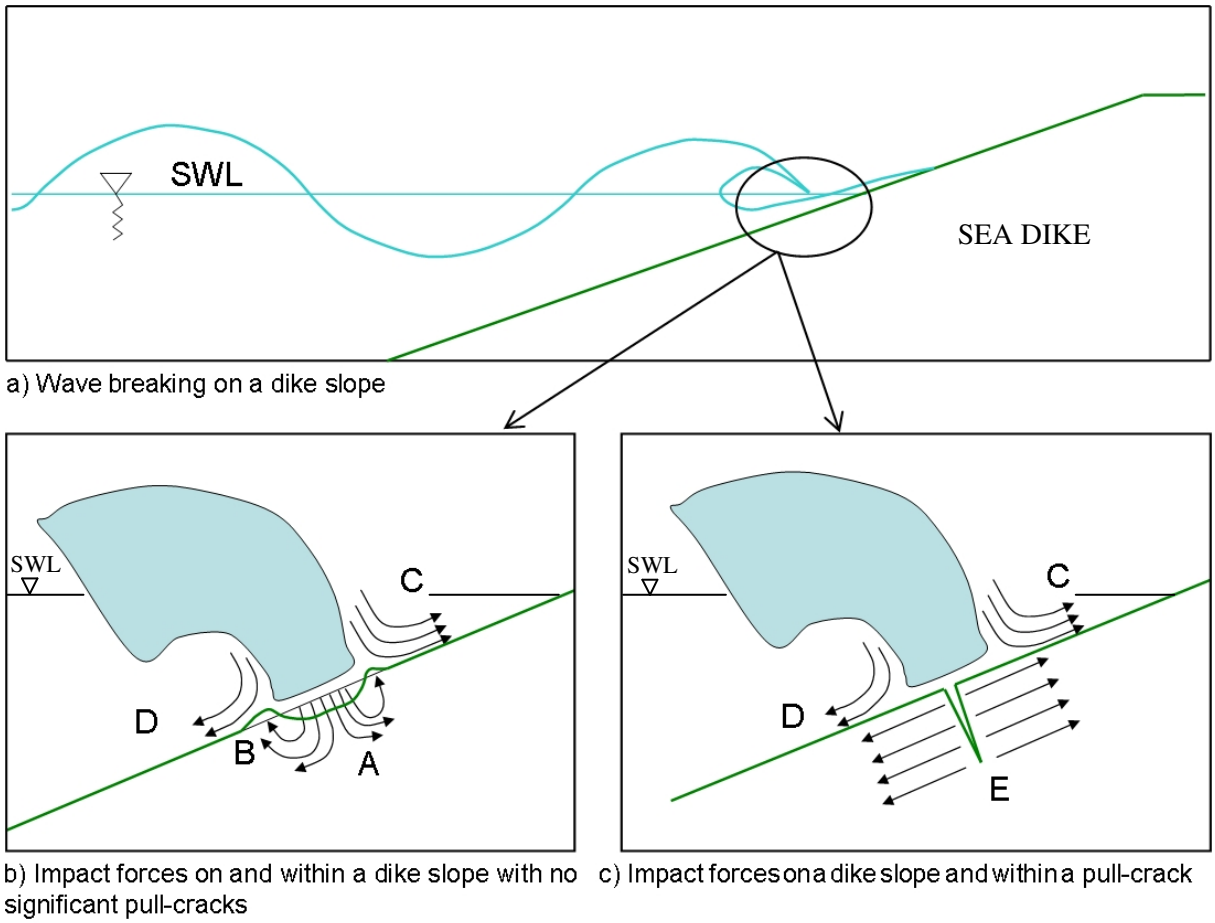

Figure 4: Impact forces on and within a dike slope

2.1.1 Compacted clay with no significant pull-cracks

The damage of the clay revetment related to the first mechanism, i.e due to the direct action of impact pressures on the surface of the slope (Force A in Fig.4b) was investigated in large-scale tests on clay performed in the Delta Flume and described by Delft Hydraulics (1992). The results of those tests indicate that this type of erosion was the main cause of damage induced by waves of at least 1 m significant height (H_S) in normally erosion-resistant clay. In a relatively short time, holes deeper than 0.8 m can form in clay without a grass cover, but the report suggests that actually this form of erosion probably never occurs with waves of less than H_s=0.5m.

Large-scale tests were performed also with a dike slope of 1:4 protected by a clay revetment with grass cover using waves of 1.5m (Smith et al, 1992). In these tests, small, local damage of the grass cover occurred after more than 16 hours of wave loading. A serious damage of the clay cover occurred only after the grass sod on the clay had been severely affected. In general, it was suggested that high waves can cause damage in a short time in the zone about mean high water level only in clay without grass. Low waves can only cause damage in poorly erosion-resistant clay when it is not adequately protected by a proper revetment.

In order to obtain a formula to calculate the amount of soil that is eroded due to single breaking wave impact, one may use the similarities to "splash erosion" considered in case of erosion due to the impact of a water mass with known kinetic energy. For this purpose, the following, empirical formula proposed by Woolhiser et al. (1990) may be used:

$$R_d = k_d \cdot E_k \cdot e^{-wh} \tag{2.1}$$

with:

- R_d - volume of soil eroded after a single impact event $[cm^3]$
- k_d - empirical detachability coefficient $[cm^3/J]$
- E_k - kinetic energy of an impact event[J]
- w - empirical coefficient representing the effectiveness of a water layer to damp impact pressures $[-]$
- h - water layer thickness $[m]$

Eq.(2.1) includes all relevant parameters, such as the kinetic energy of the impact, the thickness of the water layer (strong influence on damping) and an empirical parameter describing the detachability of the soil.

2.1.2 Clay with significant shrinkage cracks

Führböter (1966) proposed the following conceptual model to calculate the effect of impact pressures acting on water-filled cracks in a clay cover: if a water-filled crack of depth *a* and length *L* (the width and geometry of the crack are not considered) is subjected to an impact pressure p_{max} then the pressure is instantly (speed of sound in water c=1485m/s = speed of pressure propagation) transferred fully to the two side walls of the crack. The force acting on the wall of the crack is then calculated as follows (see also Fig.5):

$$F_{crack} = p_{max} \cdot a \cdot L \tag{2.2}$$

with:

- F_{crack} - force acting on the wall of crack $[N]$
- a - depth of crack $[m]$
- L - length of the crack $[m]$
- p_{max} - maximum impact pressure $[Pa]$

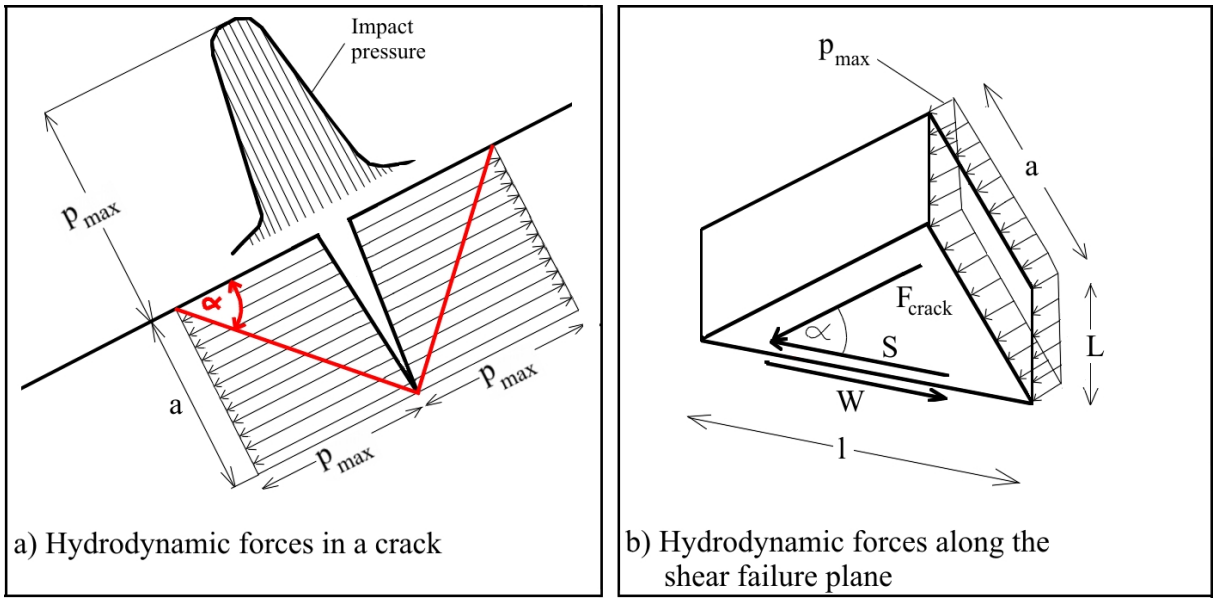

Figure 5: Forces inside a crack subjected to an impact pressure

These forces are absorbed by the compression and the shear strength of the soil behind the walls of the crack. The weight of the soil body is considered by Führböter (1966) to be negligibly small in comparison to the possible impact forces. Using this assumption, only the shear strength provided by cohesion c of the soil acts as a resistance.

The shear stress acts on a plane leaning to the surface with an angle α and provides the following shear force (see Fig.5b):

$$S = a \cdot L \cdot p_{max} \cdot cos\alpha \tag{2.3}$$

the resistance force is provided by the shear strength described by cohesion c :

$$W = l \cdot L \cdot c \tag{2.4}$$

setting

$$l = \frac{a}{sin\alpha} \tag{2.5}$$

gives

$$W = \frac{a \cdot L \cdot c}{sin\alpha} \tag{2.6}$$

Solving the limit state equation $S = W$ for $sin\alpha$ provides the angle of shear failure α :

$$sin\alpha = \sqrt{\frac{1}{2} \pm \sqrt{\frac{1}{4} - (\frac{c}{p_{max}})^2}} \tag{2.7}$$

which leads to p_{max}=2c as the critical impact pressure, i.e. the shear failure occurs for impact pressures p_{max} greater or equal to twice cohesion 2c.

The extended approach by Richwien (2003) considers also the forces that were neglected by Führböter (1966), such as the weight of the soil body G, the reaction of the soil Q and the pore water pressure U,

but it provides only very rough information on the possibility of failure as it is based on a simplified, graphical analysis of forces. This approach is based on the analysis of all the forces that provide resistance. Maximal force that can be absorbed by soil without failure (S_{poss}) is obtained as the line that closes the polygon of resisting forces. Two cases are considered (Fig.6):

- all forces act simultaneously - the force that can be absorbed by the soil (S_{poss}) is significantly larger than the mobilising force S - no failure occurs (Fig.6b);

- there is a slight time shift between the forces S and P - The force that can be absorbed by the soil is in this case significantly smaller - a shear failure may occur - (Fig.6c). The same process takes place when the soil has lost cohesion, due to infiltration, for instance.

Although this conceptual model considers all resisting and mobilising forces, it is very difficult to apply it into a model for the prediction of shear failure in a crack subjected to impact pressures. The main difficulties are:

- One of the main assumptions states, that the excess water pore pressure *U* and the resulting soil reaction *Q* occur together with the impact pressure *P*. In fact, there is a time shift between those forces. At the moment, no methods are available for the estimation of this value.

- All forces except the impact pressure in the crack depend on the shape of the mobilised soil block, that again depends explicitly on the unknown angle of shear failure α - as a result, only a complex, iterative solution can be applied;

- The time shift between the forces P and S is needed as an input data. In fact, the same problem was solved in the approach of Führböter (1966), assuming that the time shift between forces P and S occurs for every impact event and the shear failure occurs within the short time period, when no impact pressure is no more present on the surface, but is still present within a crack.

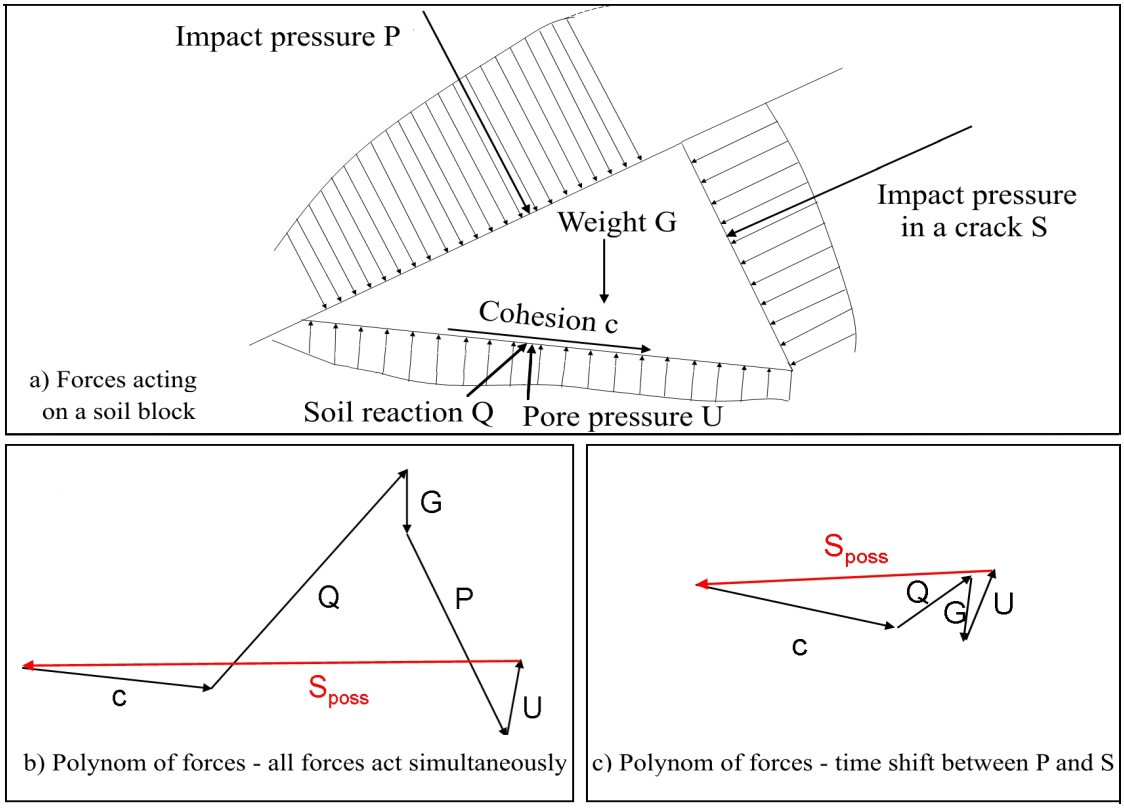

Figure 6: Forces on a soil body with crack subjected to an impact pressure: Richwien's extension of Führböter's model

The conceptual model of Führböter and its extension by Richwien are based on idealized conditions. In reality, the cracks are filled with an air-water mixture. This mixture, due to the presence of air bubbles indicates significantly increased compressibility compared to pure water, which results in a higher rate of energy dissipation (pressure damping) and decreased velocity of pressure propagation (50-300 m/s). Furthermore, the width of the crack is not considered, but according to literature Müller et al, (2003) it also plays a role, mainly due to the dependency of the air content of the water-air mixture on the crack width.

2.2 Effect of grass roots on the properties of the soil

As the clay used in sea dikes is commonly reinforced with a grass cover, it is necessary to investigate also the effects of grass roots on the erosion resistance and shear strength of soil. Only one model describing the root reinforcement is available (Wu et al, 1979) , showing that the increase in the shear strength of the soil (so-called *apparent root cohesion* c_R) due to the bonding action of grass roots can be calculated as (Fig.7) :

$$c_R = T_R \frac{V_R}{V}(cos\theta \cdot tan\phi + sin\theta) \tag{2.8}$$

where:

- T_R - root tensile strength [N/ m^2]
- V_R - volume of roots in the soil [m^3]
- V - total volume of soil [m^3]
- θ - root angle of shear rotation [^{0}]
- ϕ - internal friction angle of the soil [^{0}]

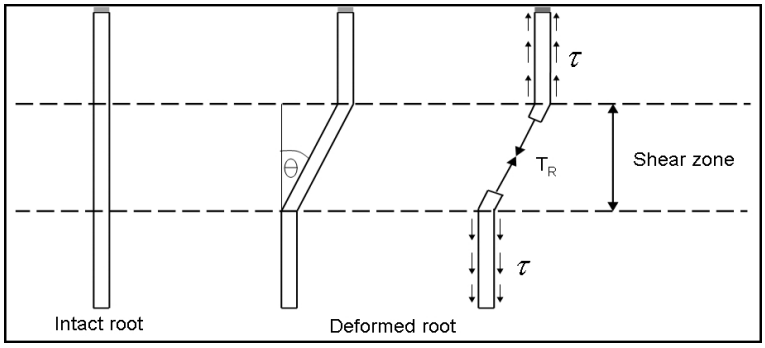

a): Flexible elastic perpendicular root reinforcement - principle sketch (Wu et al, 1979)

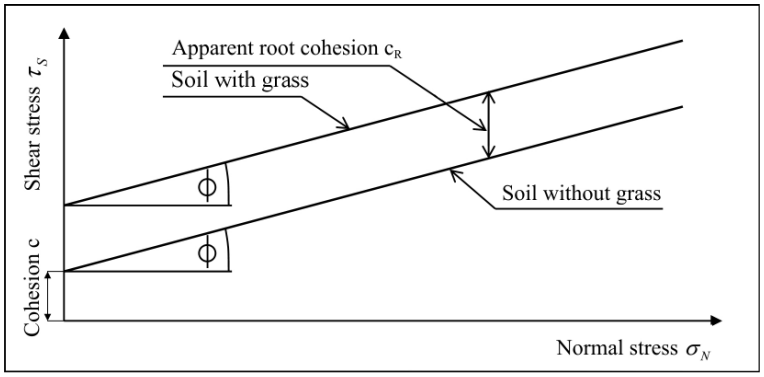

b) influence of the apparent root cohesion on the shear strength of soil

Figure 7: Grass root reinforcement of soil and apparent root cohesion (adopted from Wu et al, 1979)

The main parameters involved in Eq.(2.8) may be briefly described as follows (see also Young, 2005):

- *Tensile strength (T_R)*
  Various authors (Simon and Collison, 2001 or Cazzuffi and Crippa, 2005) state that root tensile strength has a negative exponential distribution with respect to root diameter. However it should be noticed, that none of the authors has presented root diameter distribution function. Instead, average root diameter of the range given for some grass species is used to obtain the root tensile strength. The measured tensile strength of roots for different types of grass may vary in the range 1.3-56 MPa depending on the grass species, mean root diameter and the season of the year (Young, 2005)

- *Proportion of grass roots and the soil volume V_R/V*
  The proportion of roots in a given soil body is described by the root volume ratio. Cazzuffi and Crippa (2005) state that although it is obvious that the root volume ratio decreases with depth, there are no detailed investigations on the decrease function. The aforementioned authors suggested that either a linear or exponential function might be used for this purpose. Sprangers (1999) has investigated the dependency of the root volume ratio on the depth under the surface for 24 dike grasslands in the Netherlands. Regression analysis was used to fit eighteen different functions. The one that is considered to provide the best fit is the exponential function presented in Fig.8.

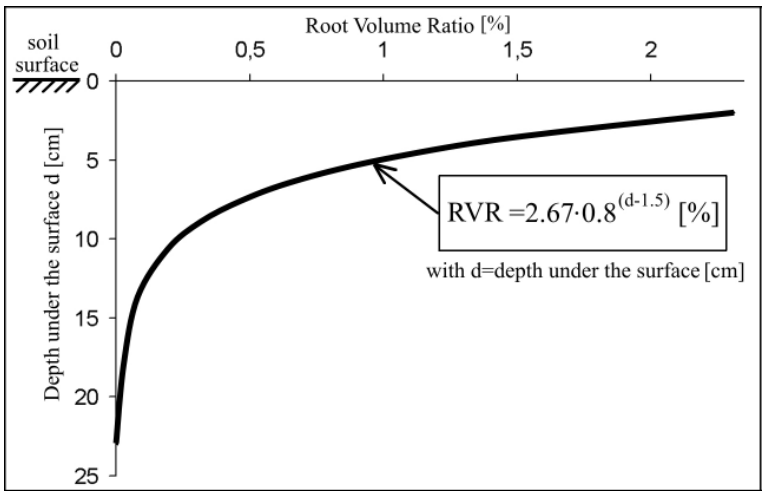

Figure 8: Dike grassland - Root Volume Ratio as a function of depth under the surface for dike grass (after Sprangers, 1999)

- *Root angle of shear rotation θ*
  Very little information is available on the values of the root angle of shear rotation θ (the angle at which the root will break). Wu et al. (1979) suggested a range of 45^0 to 70^0 from field observations of conifers, however it is unknown if any similarity to dike grasses exists. Young (2005) suggests that for grassland θ should be very close to the upper limit of 70^0.

It should be emphasised that although some laboratory experiments on the erosion resistance of grass cover against breaking wave impacts have been conducted (Smith et al., 1994), they provide only basic information on the processes that lead to damage of the revetment. Furthermore, neither the formula of Führböter (1966) nor the extended approach of Richwien (2003) for the failure of a dike revetment due to impact pressures in the crack of a soil body has been verified experimentally. Therefore, it is not clear whether the assumptions of these approaches are justified.

The formula of Woolhiser et al (1990) for the prediction of the surface erosion was verified only for a narrow band of input conditions. It is therefore necessary to perform experimental tests in order to check the applicability of this approach also in case of sea dikes subject to breaking wave impact.

The approach of Wu et al. (1979) to calculate the reinforcement of soil by a root network has never been tested on grass. Furthermore, no detailed information on the influence of the root volume ratio on the progress of erosion due to impact pressures is available.

In order to shed some light on all those problems, experimental tests on clay with and without vegetation were performed at the Leichtweiß-Institute for Hydraulic Engineering and Water Resources, TU Braunschweig.

3. Laboratory Experiments

3.1 Objectives

The laboratory experiments were conducted in six phases divided into two parts:

First part: soil laboratory tests on the samples of clay cover with and without vegetations performed in order to describe the parameters of root network and its influence on the soil geotechnical properties:

1. phase - Tests on the grass cover in order to describe the distribution of root density over the soil depth under the surface of the dike and to evaluate the quality of the tested grass cover;

2. phase - Tests on the grass cover in order to investigate the influence of vegetation on the shear strength of the soil. The applicability of the model proposed by Wu et al.(1979) is analysed;

Second part: tests on erosion resistance of the clay cover with and without vegetation performed using a wave impact simulator:

3. phase - Clay samples with an artificial crack are subject to controlled impact pressures in order to investigate the process of shear failure of the soil. This should also allow to confirm and eventually modify the model of Führböter (1966) described by Eq.2.7 or its extended version by Richwien (2003) as described in Figure 6;

4. phase - Tests on the effects of impact pressures acting on a crack in clay with vegetation in order to check whether the conceptual model of Führböter (1966) also applies for reinforced soil;

5. phase - Tests on compacted clay without pull-cracks subject to the repeated action of impact pressures in order to analyze the processes that lead to surface erosion of the soil. The applicability of the formula proposed by Woolhiser et al. (1990) is investigated and coefficients of Eq. 2.1 are calibrated;

6. phase - Tests on clay cover with intact vegetation subject to the repeated action of impact pressures in order to examine the erodibility of grass-reinforced clay cover due to repeated action of impact pressures. Furthermore, the influence of root volume ratio V_R/V on the erodibility of soil will also be investigated.

3.2 Soil Laboratory Tests

Before embarking into the performance of the tests of soil samples using the wave impact simulator, it is necessary to evaluate their geotechnical properties.

The following samples are tested:

- **Samples of a clay cover with grass** from a prototype sea dike "Alter Störtebeker Deich" in Leybucht, Germany. No information on the grass characteristics were provided, important parameters of vegetated cover are to be determined during the laboratory tests.
- **Three samples of clay** taken from the following locations in Germany are used (Tab.2):

  - sea dike in Cäciliengroden
  - sea dike in Elisabethgroden, km 9.0
  - sea dike in Elisabethgroden, km 3.5

Table 2: Properties of the three clay types used in the laboratory tests (IGBFT,2001)

Characteristic value	Cäciliengroden	Elisabethgr., km 9.0	Elisabethgr., km 3.5
Clay percentage [%]	35	20	10
Silt percentage [%]	53	45	30
Sand percentage S_p [%]	12	35	60
Proctor density [g/cm^3]	1.458	1.643	1.835
Permeability coeff. k_f [m/s]	$1.37 \cdot 10^{-9}$	$1.22 \cdot 10^{-8}$	$3.23 \cdot 10^{-6}$
Decomposition time $t_{30\%}$ [s]	>259200	97263	562
Plasticity index I_p [-]	0.45	0.2706	0.0649
Undrained Cohesion[kPa]	22.6-70.7	18.6-40.0	8.6-24.1
Liquidity limit w_l [-]	0.77	0.41	0.25

The samples of soil used in the tests are evaluated using the following approaches:

1. Classification number N proposed by Weißmann (2003):

$$N = \sqrt[n]{B_1, B_2, B_3 ... B_n} \tag{3.4}$$

where:

- N - classification number [-]
- B_n - classification factors [-]

Table 3: Classification of soil according to the classification number N

Classification number N	Quality of clay	Applicability class
$1.00 \le N \le 0.85$	Very good	1
$0.85 \le N < 0.75$	Good	2
$0.75 \le N < 0.65$	Moderate	3
$0.65 \le N < 0.50$	Weak	4
$N < 0.50$	Bad	5

The classification factors essentially depend on the soil properties and are calculated as:

- B_1 - permeability coefficient k_f

$$B_1 = 0.7 - \frac{(\log k_f + 4)}{20} \tag{3.5}$$

- B_2 - decomposition time $t_{30\%}$

$$B_2 = 0.2 \cdot \log(t_{30\%}) \tag{3.6}$$

- B_3 - shrinkage V_s

$$B_3 = 1.0 - 1.25 \cdot (V_s - 0.05) \tag{3.7}$$

- B_4 - plasticity index $I_p = w_l - w_p$ (w_l and w_p are liquidity and plasticity limits, resp.)

$$B_4 = 0.3 + 2 \cdot (w_l - w_p) \tag{3.8}$$

The classification numbers B_n for the three soil samples described in Tab.2 are calculated using Eqs. 3.5- 3.8 and are given in Tab.4.

Table 4: Classification factors B_n for the three soil samples in Tab.2 (Weißmann, 2003)

Classification factor		Cäciliengr.	Elisabethgr.,9.0	Elisabethgr.,3.5
B_1	Permeability coeff.	0.95	0.91	0.77
B_2	Decomposition time	1.0	1.0	0.50
B_3	Shrinkage	0.75	0.75	0.87
B_4	Plasticity index	1.0	0.7	0.2

The classification numbers according to Eq.(3.4) for each type of clay are as follows :

- Cäciliengroden:

$$N_C = \sqrt[4]{0.95 \cdot 1.0 \cdot 0.75 \cdot 1} = 0.88 \Rightarrow \text{very good clay}$$

- Elisabethgroden, km 9.0:

$$N_{E,9.0} = \sqrt[4]{0.91 \cdot 1.0 \cdot 0.75 \cdot 0.7} = 0.83 \Rightarrow \text{good clay}$$

- Elisabethgroden, km 3.5:

$$N_{E,3.5} = \sqrt[4]{0.77 \cdot 0.5 \cdot 0.87 \cdot 0.2} = 0.51 \Rightarrow \text{weak clay}$$

2. Dutch approach for the classification of clay for sea dikes according to the erosion resistance of clay for dikes (TAW,1996)

Table 5 shows the requirements that must be checked during the evaluation of clay to be used for sea dikes, within the following categories:

- Category 1. Erosion resistant;
- Category 2. Moderately erosion resistant;
- Category 3. Little erosion resistance.

The distinction between the three categories is based on the Atterberg limits and the sand content.

Table 5: Classification of clay for dikes according to the Dutch requirements (TAW,1996)

Category	w_l [-]	I_p [-]	Sand content S_p [%]
1	>0.45	>0.73 · (w_l-20)	<40
2	<0.45	>0.18	<40
3	-	<0.18	>40

The three soil samples in Tab.2 are therefore classified as follows:

- Cäciliengroden :
$$w_l = 0.77,\ I_p = 0.45,\ S_p = 12\% \ \Rightarrow \text{Category 1}$$
- Elisabethgroden, km.9.0:
$$w_l = 0.41,\ I_p = 0.208,\ S_p = 35\% \ \Rightarrow \text{Category 2}$$
- Elisabethgroden, km. 3.5:
$$w_l = 0.25,\ I_p = 0.06,\ S_p = 60\% \ \Rightarrow \text{Category 3}$$

Both proposed approaches provide a comparable classification of the three types of clay used in the experiments. Each soil type represents a different category of erosion resistance. The soil sample taken at the location Cäciliengroden represents the **strong clay**, the sample taken at the location Elisabethgroden , km 9.0 represents the **moderate clay**, while the soil sample from the location Elisabethgroden , km 3.5 represents the **weak clay**.

3.2.1 Measurements of the Root Volume Ratio and estimation of the grass cover quality

In order to evaluate the quality of a grass cover and to investigate the influence of the root network on the strength of reinforced soil, the knowledge of root percentage in the soil sample is needed. The soil laboratory tests to obtain the root volume ratio RVR were performed at the Leichtweiß-Institute using the following procedure:

1. a sample of the grass cover is extracted from a sea dike (see Section 3.2.2 for details) using a steel pipe of inner diameter of 48mm inserted perpendicularly to the surface of the dike up to the depth of 20cm;

2. the extracted, cylindrical sample is cut into slices of 2cm thickness. Each slice represents a given depth under the surface and is used to provide an information on the RVR for this particular depth;

3. for every single slice the roots are separated from the soil and carefully cleaned with water

4. the roots are dried in oven using a temperature 105° C for 24 hours

5. the dry mass of roots m_R separated from each single slice is obtained. The density of dry grass roots ρ_R is known (ρ_R=300 kg/m^3 (Young, 2005)). The volume of roots V_R in a single slice is calculated as:
$$V_R = \frac{m_R}{\rho_R} \tag{3.9}$$

6. the root volume ratio RVR is calculated as:
$$RVR = \frac{V_R}{V_{ss}} \cdot 100\ [\%] \tag{3.10}$$

where V_{ss} is the total volume of a single slice, including the roots ($V_{ss} = 36.2cm^3$)

7. the same procedure is repeated 10 times, using samples extracted at different locations on the dike slope.

The results of all the ten measurements as well as the mean value of root volume ratio for each depth are summarized in Table 6.

Table 6: Measured root volume ratio for the ten samples taken from the dike.

Depth [cm]	Root Volume Ratio RVR [%]										RVR Mean [%]
2,00	2,43	0,99	0,96	1,45	0,50	0,77	3,28	1,93	2,15	1,35	1,58
4,00	1,82	0,50	0,48	0,73	0,26	0,56	0,36	0,71	1,07	0,67	0,72
6,00	0,91	0,73	0,31	0,31	0,76	0,28	0,17	0,36	0,64	0,99	0,55
8,00	0,52	0,36	0,15	0,15	0,38	0,36	0,13	0,17	0,31	0,50	0,30
10,00	0,26	0,86	0,09	0,21	0,07	0,17	0,07	0,09	0,10	0,16	0,21
12,00	0,03	0,43	0,05	0,10	0,03	0,10	0,01	0,06	0,05	0,08	0,10
14,00	0,01	0,07	0,01	0,00	0,00	0,05	0,00	0,03	0,13	0,03	0,03
16,00	0,01	0,03	0,00	0,00	0,00	0,00	0,00	0,00	0,00	0,01	0,01

A comparison of root volume distribution measured in the laboratory tests with the mean distribution measured for 24 Dutch dikes and reported by Sprangers (1999) is shown in Figure 9. A good agreement between these two distributions can be observed. It will be therefore assumed, that the grass sample represents the typical grass cover of moderate quality. The best fit function that will be used for the purposes of further tests reads:

$$RVR = A \cdot D^{(d-2)} \ [\%] \tag{3.11}$$

where A and D are empirical coefficients that depend on the quality of grass cover while d is the depth under the surface given in centimetres. The coefficients A and D are supposed to decrease with the clay quality, as stronger clay prevents the growth of a dense root network. For the tested samples of grass cover the coefficients are of the value A=1.58 and D=0.75.

The second important parameter that describes the quality of the root network is the tensile strength of the roots. The tensile strength of ten single roots was measured, the obtained values are in a quite narrow range 300-800 N/cm^2, with mean of T_R=500 N/cm^2.

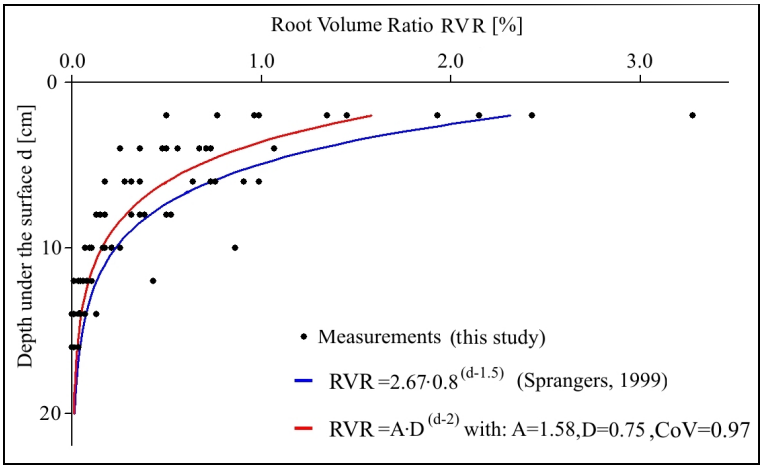

Figure 9: Measured root volume ratio for the samples taken from the dike

3.2.2 Direct shear tests with grass cover (shear strength)

The next laboratory tests are performed in order to examine the influence of grass roots on the shear strength of the soil. The distribution of roots for the investigated grass layer has been measured, the knowledge of the shear strength of the reinforced soil at different depths under the surface of the dike is needed. To achieve this goal, direct shear measurements are performed with the shear plane set to 2,4,6,8 and 10 cm under the surface (Fig.10)

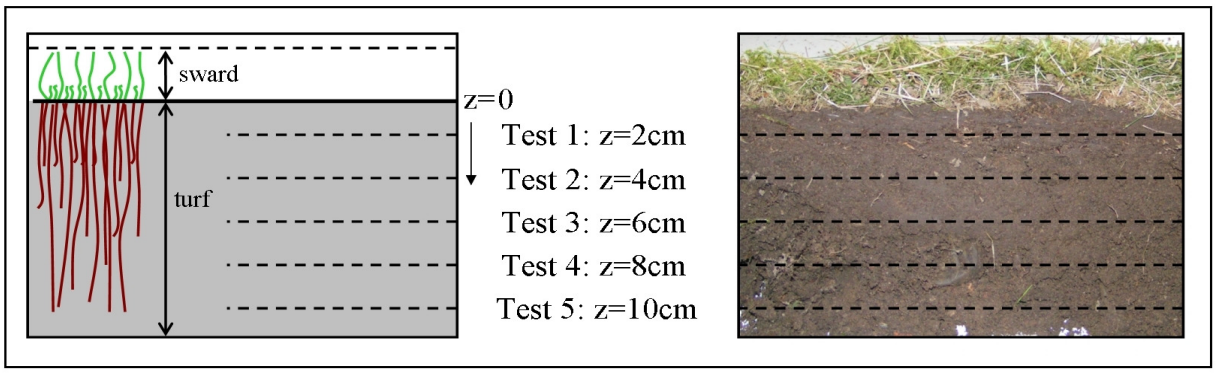

Figure 10: Planes of shear strength measurements

For comparison, the tests on the sample of the same soil but without grass are performed. Measured cohesion of the soil c_s=7 *kN/m*^{2}. The results are summarized in Table 7.

Table 7: Results of the direct shear tests

Test no.	Depth *d* [cm]	Cohesion [kN/m^2]		
		Clay	Clay with grass	Grass contribution (apparent root cohesion)
1	2	7	101	94
2	4	7	49	42
3	6	7	24	31
4	8	7	17	24
5	10	7	7	14

The comparison of measured values with the increase of shear strength of the reinforced soil (apparent root cohesion) calculated using Eq. (2.8) is summarized in Figure 11.

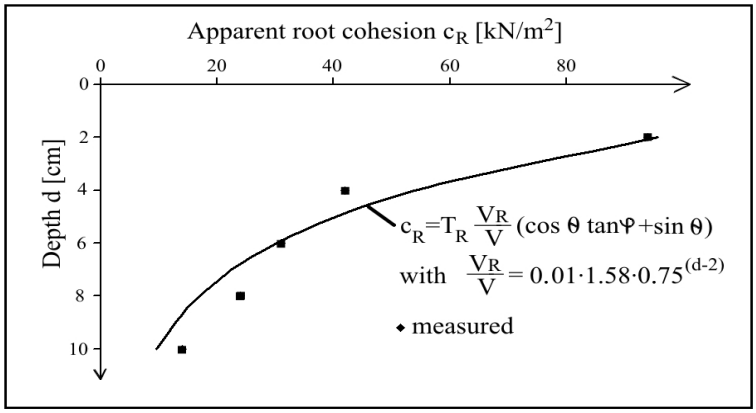

Figure 11: Measured and calculated increase of shear strength

Overall it can be stated that the root reinforcement model (Eq.(2.8)) proposed by Wu et al. (1979) shows good agreement with the experimental. Therefore, it can be applied in the case

of dike breaching model for the calculation of shear strength of root reinforced soil as a function of the depth under the slope surface.

3.3 Set-up and procedure for the tests with wave impact simulator

3.3.1 Experimental set-up for the generation and evaluation of impact pressures

The experimental set-up developed and described by Pachnio (2005) has been used (see Fig.12). It consists of a vertical pipe that is used to contain a given mass of water to be suddenly dropped from a given fall height h_f. The pipe can be placed in a range of h_f=50cm up to h_f=165cm above the soil sample. A computer controlled system fills the pipe with a given amount of water and releases the mass using a pneumatic-steered valve. The falling mass of water hits the soil sample generating an impact pressure. The dependency upon the fall height of the pressures at the surface of the soil sample and within a crack was measured and described by Pachnio (2005). Therefore, the values of the impact pressures and energy will not be directly measured but only calculated as follows (Pachnio, 2005):

- impact pressure $$p_{max} = \frac{2 \cdot h_w \cdot \rho \cdot \sqrt{2 \cdot g \cdot h_f}}{\Delta t} \quad (3.1)$$

- impact energy $$E_k = m \cdot g \cdot h_f \quad (3.2)$$

where (see Figure 9):

- h_w - water depth in pipe (here $h_w = 0.25m$)
- m - mass of water (here m=2kg)
- Δt - time of the total impact pressure duration
- h_f - fall height of the water mass
- ρ - water density

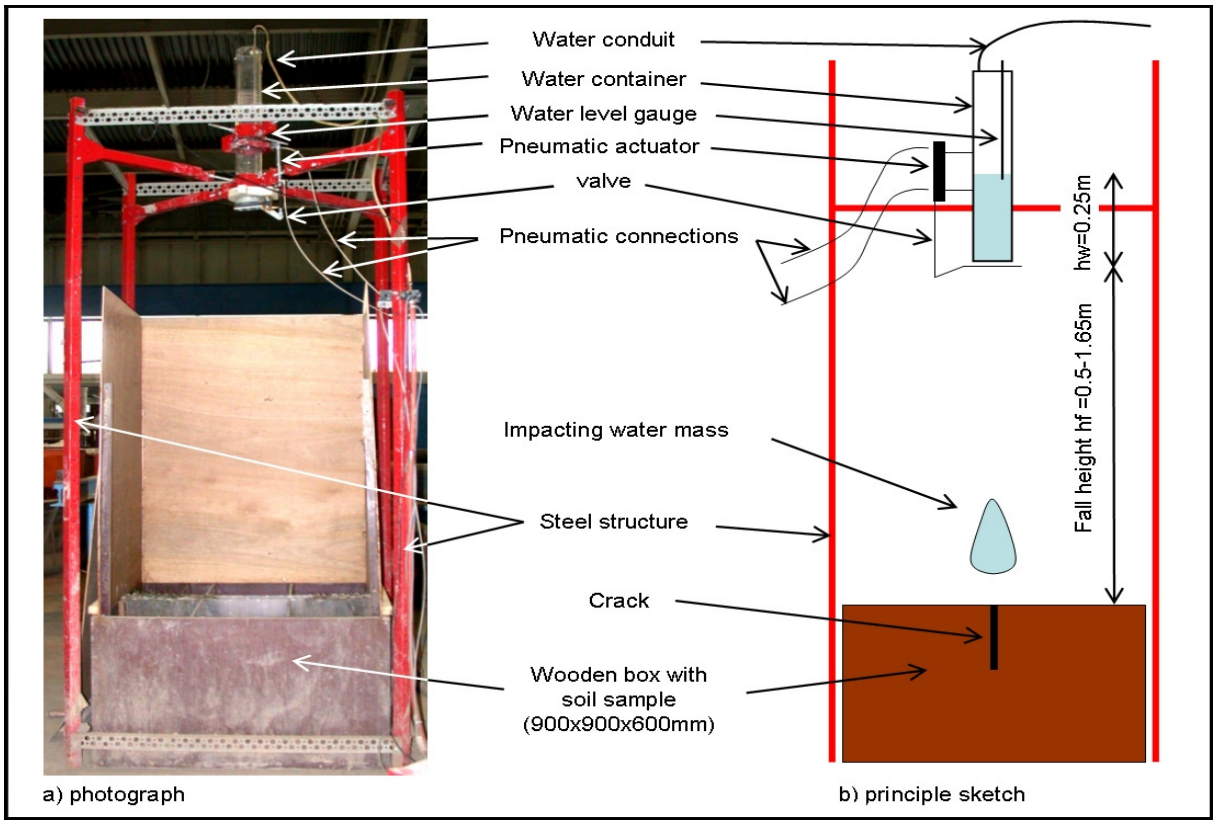

Figure 12: Experimental set-up for impact tests

3.3.2 Soil samples and their preparation

Wooden boxes of dimensions 900x900x600mm, as described by Pachnio (2005) are used in the experiments, but they have been slightly modified in order to provide a better insight on the processes taking place under the surface of the soil sample. This is achieved using two transparent walls within the box, (Figs.13 and 14).

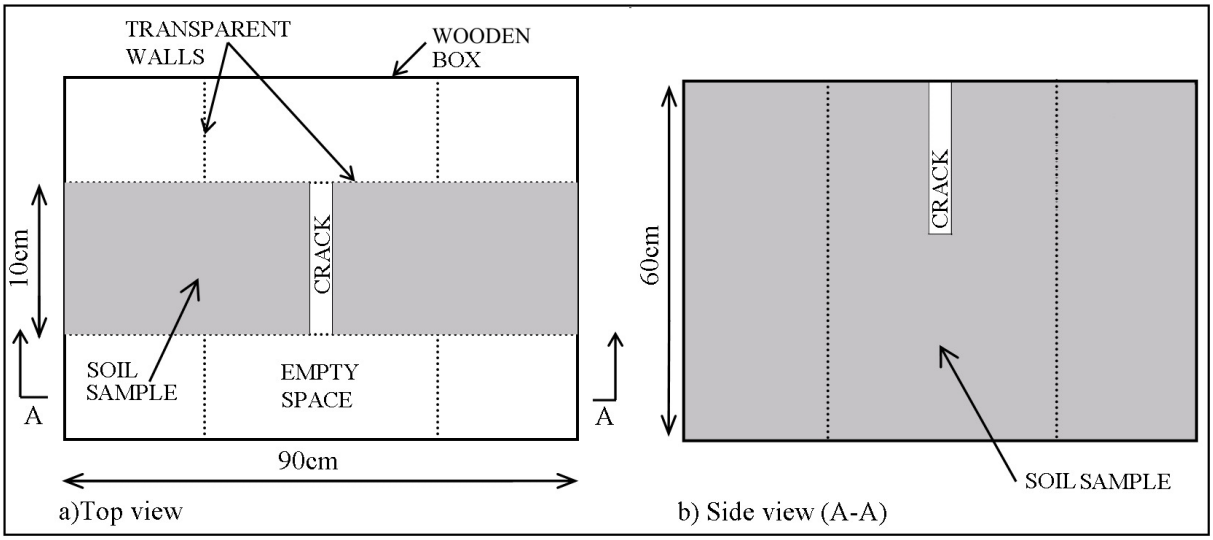

Figure13: Box used in laboratory tests and clay sample with crack

Figure.14: Box used in tests

3.3.3 Tests with clay sample including an artificially induced crack

In order to investigate the effects of impact pressure acting on the soil with a water-filled crack the laboratory tests were performed at the Leichtweiß-Institute using the experimental set-up described in Section 3.3. All tests were performed using the following procedure:

1. The clay is placed into a box (see Section 3.3.2) in six layers with a 10cm thickness. Each layer is compacted using a force generating constant pressure of about 100 kPa.

2. After all layers have been compacted, a crack is artificially induced in the middle of the sample, at the location where the falling water mass hits the soil. The crack is 150 mm deep, 10 mm wide and 100 mm long. In Fig.15 the side and top views of the crack are shown.

   a) side view

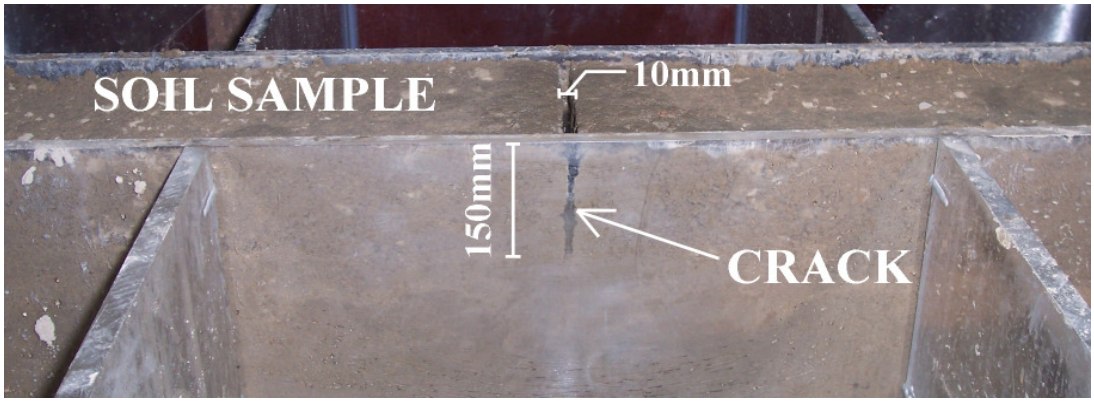

   b) top view

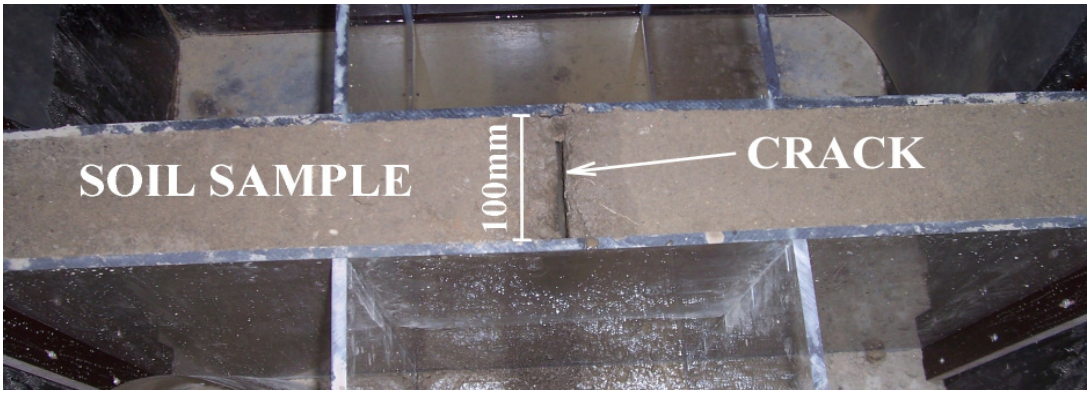

Figure 15: Artificial crack in the soil sample - side and top views

3. the crack is filled up with water.

4. the automatically released mass of water (see Figure 12) is used to produce an impact pressure in the crack at the surface of the sample (see Fig.16). No pressure measurements are needed, as the dependency of pressure on the drop height and

mass of the falling water is known (see Eq.3.1)

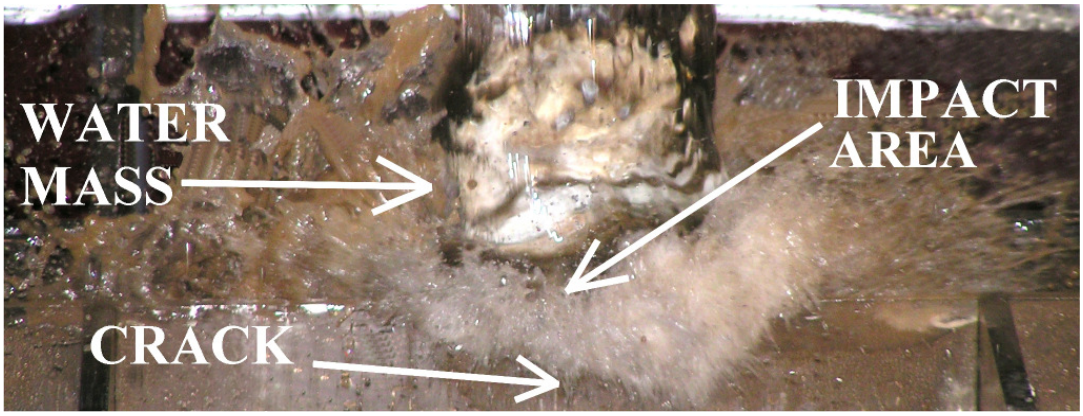

Figure 16: Mass of water impacting the sample - side view

5. After an impact event for which shear failure occurred, a picture of the crack development is taken, then the angle of shear failure α (Fig.5 and Fig.17) between the failure plane and the surface of the soil sample is measured

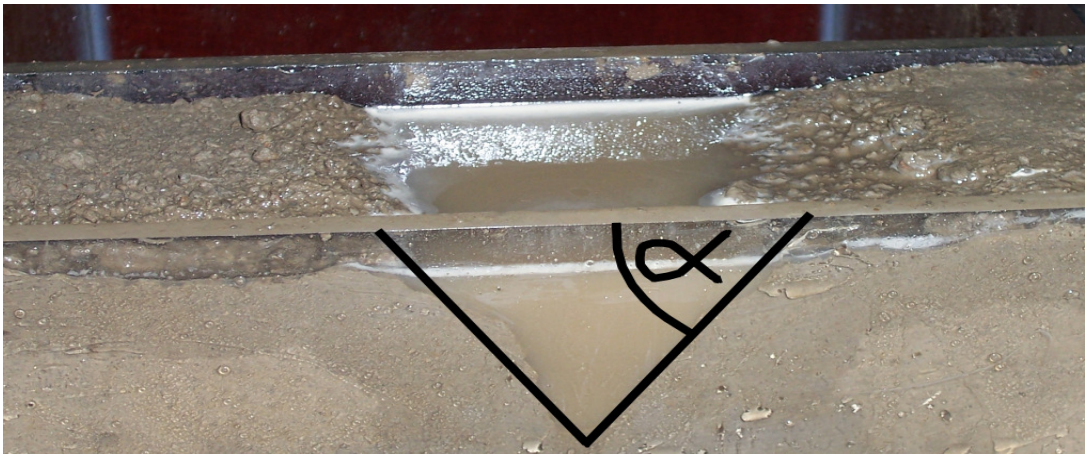

Figure 17: Crack development recorded after an impact - angle of shear failure α

6. For every single test a soil sample is taken in order to measure the water content w_c This represents an indirect measurement of the shear strength, as an empirical equations for the calculation of shear strength depending on the water content for every type of tested soil are provided:

- Weak clay:

$$\tau_s = 2550 \cdot e^{-33 \cdot w_c} [kN/m^2] \quad (3.12)$$

- Moderate clay:

$$\tau_s = 2800 \cdot e^{-20 \cdot w_c} [kN/m^2] \quad (3.13)$$

- Strong clay:

$$\tau_s = 7230 \cdot e^{-12 \cdot w_c} [kN/m^2] \quad (3.14)$$

The graphical interpretation of Eqs. 3.12-3.14 is provided in Fig 18.

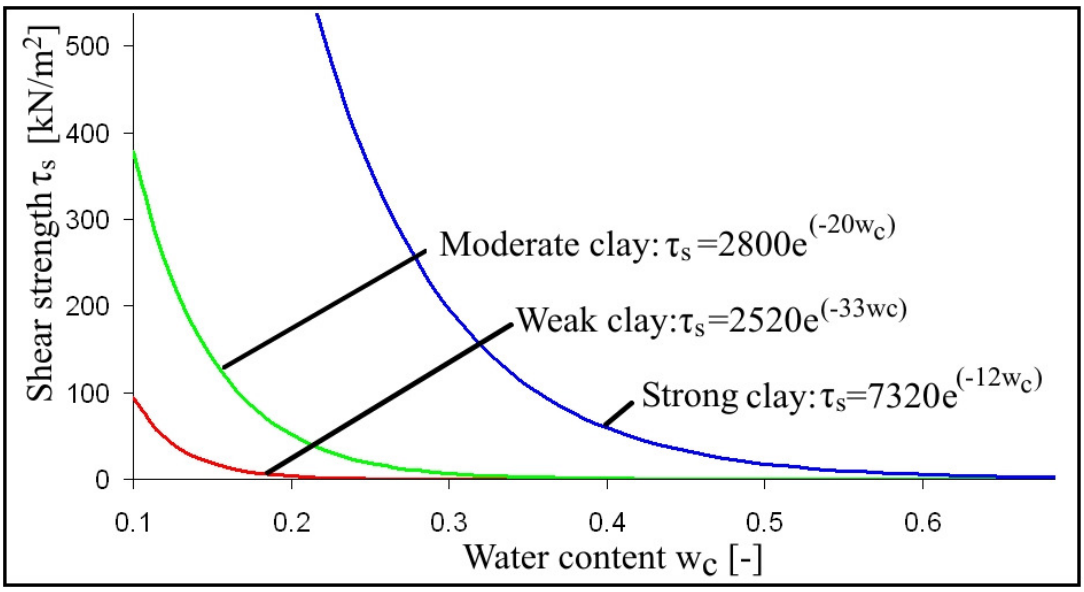

Figure 18: Dependency of shear strength on water content (after Kortenhaus, 2003)

The laboratory tests programme on the effect of impact pressures in a water-filled crack within a soil sample is summarized in Table 8:

Table 8: Test programme for the compacted clay with an artificially induced crack

Clay	Fall height h_f [cm]	Impact pressure [kPa]	Number of tests
Weak	50	13.62	5
	75	16.68	5
	100	19.26	5
	125	21.53	5
	165	24.74	5
Moderate	50	13.62	5
	75	16.68	5
	100	19.26	5
	125	21.53	5
	165	24.74	5
Strong	50	13.62	5
	75	16.68	5
	100	19.26	5
	125	21.53	5
	165	24.74	5
Total number of tests:			75

3.3.4 Tests with grass cover including an artificially induced crack

The main purpose of these laboratory experiments is to investigate the shear failure that may occur when a crack in grass cover is subject to impact pressures. Essentially the same procedure as in the case of clay without grass (Section 3.3.3) is applied. However, as the shear strength of the grass cover is significantly larger that the shear strength of the clay, no shear

failure should occur according to Eq.(2.7). Therefore, the tests will be performed first with the largest impact pressures. If no shear failure occurs in the grass cover with a crack subjected to the largest impact pressure that can be generated by the experimental set-up, the tests with smaller impact pressures will be abandoned.

Table 9: Tests programme for the grass cover with an artificially induced crack

Fall height h_f [cm]	Impact pressure [kPa]	Number of tests
50	13.62	5, if applicable
75	16.68	5, if applicable
100	19.26	5, if applicable
125	21.53	5, if applicable
165	24.74	5

3.3.5 Tests with a compacted clay sample without pull-cracks

The main purpose of these tests is to gain knowledge on the surface erosion processes of the soil subject to a series of impact pressures. Furthermore, the damping effectiveness of a water layer will be investigated. To achieve these goals, the tests are performed using the following procedure.

Impact tests without a damping water layer:

1. The clay material is placed as in previous tests (in six layers with 10cm thickness)

2. A series of 50 impact pressure events are generated

3. After each series of 50 impacts, a gypsum cast of the scour hole is made

4. The volume of the cast, i.e. the volume of eroded soil, is measured

Impact tests with a damping water layer:

1. The clay is placed as in previous tests (in six layers with 10cm thickness)

2. The surface of the clay is placed 1, 2, 2.5 or 4 cm under the top of the box, depending on the test run

3. The space between the surface of the soil and the top of the box is filled up with water as a the damping layer

4. A series of 50 impact pressure events are generated. The focus is put on the damping effect of the thickness of water layer. If necessary, the space is filled up with water in order to keep the thickness of water layer constant for every single impact

5. After each series of 50 impacts, a gypsum cast of the scour hole is made

6. The volume of the cast; i.e. the volume of eroded soil, is measured

The complete test programme for the experiments with compacted clay is given in Table 10:

Table 10: Test programme for the experiments with compacted clay

Clay	Fall height h_f [cm]	Impact pressure [kPa]	Water layer thickness [cm]
Weak	50	13.62	0
			1
			2.5
	75	16.68	0
			1
			2.5
	100	19.26	0
			1
			2.5
	125	21.53	0
			1
			2.5
	165	24.74	0
			1
			2.5
Moderate	50	13.62	0
			1
			2
	75	16.68	0
			1
			2
	100	19.26	0
			1
			2
			4
	125	21.53	0
			1
			2
			4
	165	24.74	0
			1
			2
Strong	50	13.62	0
			1
			2.5
	75	16.68	0
			1
			2.5
	100	19.26	0
			1
			2.5
	125	21.53	0
			1
			2.5
	165	24.74	0
			1
			2.5
Total number of tests:			47

3.3.6 Tests with grass cover - surface erosion

The main purpose of these tests is to investigate the processes that may lead to the surface erosion of clay cover reinforced with grass when subjected to impact pressures. The focus is put on the dependency of the erosion progress on the root volume ratio. Furthermore, the damping effectiveness of a water layer will be examined. The following procedure is applied:

Impact tests with no water layer:

1. The sample of grass cover is placed in the test box, the surface of the grass is located at the same level as the top of the box
2. A series of 10 impact pressure events are generated
3. After the series of 10 impacts, the dimensions of the scour hole are measured
4. Steps 2 and 3 are repeated until the sample fails

Impact tests with water layer:

1. The surface of the grass is placed 1, 2 or 4 cm under the top of the box, depending on the test run
2. The space between the surface of the grass and the top of the box is filled up with water as a damping layer
3. A series of 10 impact pressure events are generated. The focus is put on the thickness of the water layer. If necessary, the space is filled up with water in order to keep the thickness of the water layer constant for every single impact
4. After the series of 10 impact pressure events the dimensions of the scour hole are measured
5. Steps 3 and 4 are repeated until the sample fails

The complete test programme for these experiments is summarised in Tab.11.

Table 11: Test programme for the experiments with grass

Fall Height [cm]	Impact pressure [kPa]	Water layer thickness [cm]
50	13.62	0
		1
		2
		4
75	16.68	0
		1
		2
		4
100	19.26	0
		1
		2
		4
125	21.53	0
		1
		2
		4
165	24.74	0
		1
		2
		4
Total number of tests		20

3.4 Summary

The proposed test programmes enable one to investigate in the laboratory the behaviour of a typical sea dike revetment subjected to a repeated action of impact pressures due to breaking waves. Clay with grass as a compound material and clay without grass used for dike revetments are considered. Three types of soil, representing three types of clay with different quality and properties, as well as grass of moderate quality, are used. The experimental verification of two possible failure modes that can lead to breach initiation:

- shear failure in water-filled cracks
- surface erosion

for both materials subject to impact pressures is performed using a wide range of boundary conditions. The obtained results will be used to verify and if necessary also to modify available conceptual models for surface erosion (Wu et al, 1979) and shear failure in water-filled cracks (Führböter, 1966). Furthermore, the analysis of the mechanical properties of the grass root network allows to estimate its influence on the properties of the reinforced soil.

4. Main Results of Impact Experimens

4.1 Clay sample with a pre-induced crack

The tests on clay with an artificial crack have confirmed the conceptual model of Führböter (1966) only partially. During the experiments the shear failure itself occurs, but the observed process of failure significantly differs from the predicted one. The soil from the scour hole is quarried out in the form of particles and small aggregates instead of being removed as a single soil block (see Fig.19). This form of the shear failure was observed independently on both the impact pressure and the type of the investigated soil. Furthermore, a quite large scatter of the experimental data is observed which can be explained by the inhomogeneity of a natural soil samples.

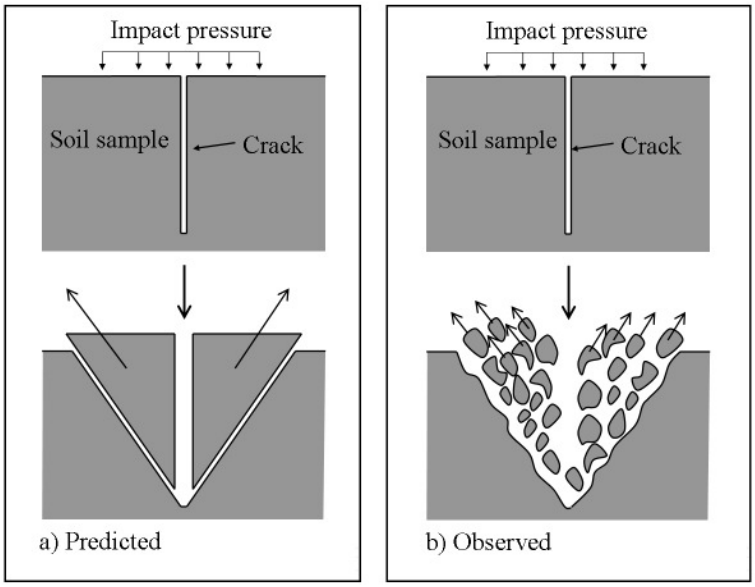

Figure 19: Predicted and observed shear failure - principle sketches

4.1.1 Weak and moderate clay

The measured angle of shear failure α_{meas} for every single test run described in Section 3.3.3 is compared with the value calculated using the model of Führböter (1966) - Eq.(2.7). The values of maximal impact pressures used in Eq.(2.7) are calculated using the formula of Pachnio (2005) - Eq.(3.1), while the cohesion of the soil is calculated according to the measured water content and Eq.(3.12) or Eq.(3.13) for weak and moderate clay, respectively. The results of the comparative analysis are summarised in Tab.A-1 and Tab. A-2.

In the case of the weak clay the agreement between the measured and calculated values of the shear failure angle α is quite good. The measured values α_{meas} are slightly (6.5%-19%) smaller than the calculated values α_{calc} which would suggest that either the resistance of the soil is generally underestimated or the resisting forces neglected by Führböter (1966) in Eq.(2.4) also affect the angle of shear failure α. A strong dependency of the relative difference $(\alpha_{meas} - \alpha_{calc})/\alpha_{meas}$ on the impact pressure is observed (no influence of cohesion is considered). With increasing impact pressure, the difference $(\alpha_{meas} - \alpha_{calc})/\alpha_{meas}$ and related scatter significantly decrease. This might suggest that the calculation of the cohesion of the weak clay is not reliable.

The analysis of the results obtained for moderate clay shows similar tendencies. For 23 of 25 test runs the measured angle of shear failure α_{meas} was smaller than the calculated one. The

underestimation of the measured values is within a wide range (5%-95%). Only for two test runs the measured angle α_{meas} was larger than the theoretical one. The overestimation is within the range 4%-33%. Those results suggest that also in the case of moderate clay the resisting forces neglected by Führböter (1966) may affect the shear failure angle α. During the tests with moderate clay no clear dependency of the relative difference $(\alpha_{meas} - \alpha_{calc})/\alpha_{meas}$ on the impact pressure p_{max} has been observed. Furthermore, no clear dependency of $(\alpha_{meas} - \alpha_{calc})/\alpha_{meas}$ on the ratio of impact pressure and cohesion p_{max}/c could be identified.

4.1.2 Strong clay

In the performed tests the cohesion of the strong clay calculated as a function of measured water content (Eq.3.14) varied in the range of $c=13 - 254\ kN/m^2$, and the ratio p_{max}/c was in the range of 0.06-1.9, i.e. $p_{max} < 2c$. Since Eq.(2.7) is not applicable in this range no shear failure would occur in any of the test runs. However, for every single test run a shear failure occurred - the predicted resisting forces of the soil were in this case significantly overestimated. It could be explained by the structure of the strong clay which is actually not homogenous. It consists mostly of hard clumps made of fine and cohesive fraction of the soil (Fig.20).

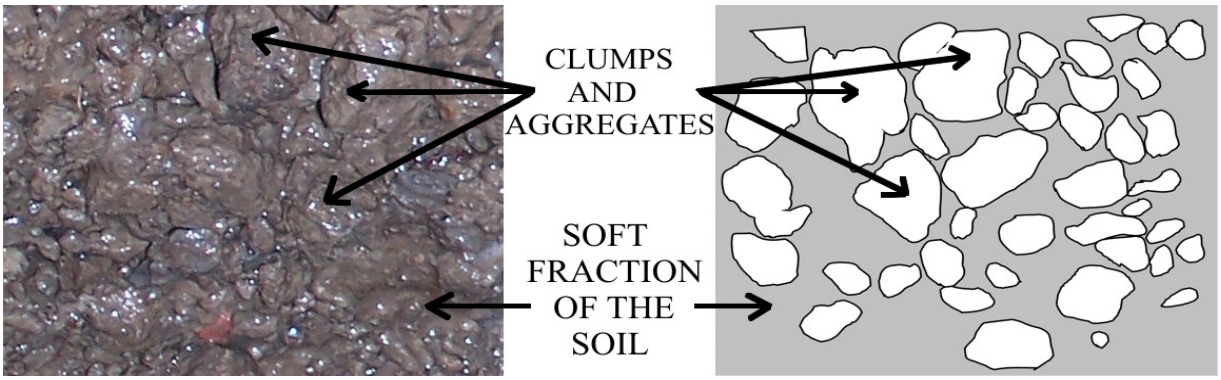

Figure 20: Structure of the strong clay tested

Although these clumps themselves are very hard, they are connected together by soft, relatively cohesionless fraction of the soil. The mean cohesion is supposed to be equal to the calculated value.

During the tests the clumps were quarried out forming a scour hole, but the failure plane run always through the weak parts of the soil body between clumps. All the measured values are listed in Tab.A-3. The obtained values of α_{meas} are in the range from 38^0 to 76.5^0 and no clear dependency of α_{meas} neither on p_{max}/c nor on p_{max} can be observed. The most probable reason for such behaviour is the already mentioned structure of the good clay.

As the distribution of the aggregates and lumps within the soil is purely random, the obtained results also show very large scatter. In Fig.21a the comparison of the measured values with the calculated ones is shown. Figure 21b presents the values excluding the area of the inapplicability of Eq.(2.7). For all soil samples the measured angle of shear failure α_{meas} is smaller than the calculated one. This suggests that either the soil cohesion is underestimated, or more probably, the neglected forces in the derivation of Eq.(2.7) affect the process of shear failure. Although the presented conceptual model of Richwien (2003) takes into consideration also the forces neglected by Führböter (1966), some of them (excess pore pressure, for

instance) have to be calculated based on the numerical simulations. Furthermore, the model itself can be solved only with the means of the iterative solution. Therefore it is suggested that, due to its simplicity, rather the model of Führböter (1966) should be improved by taking also additional resisting forces into consideration.

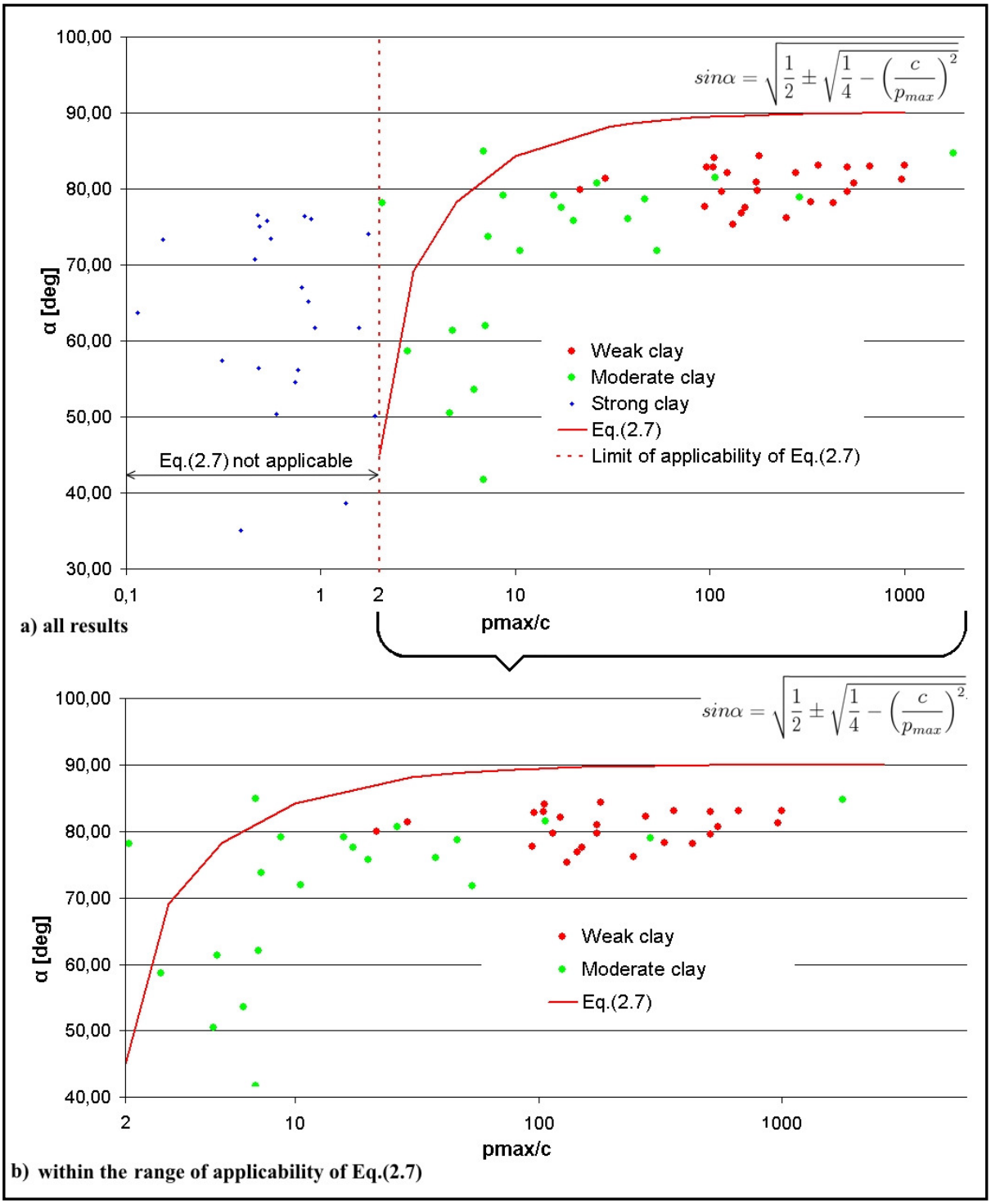

Figure 21:Summary of results

4.1.3 Improvement of the conceptual model of Führböter (1966)

As the weight of the block and the shear resistance of both sides of the block are not included in Eq.(2.7) (see Fig.22c and Fig.22d), some modifications are performed below to the model of Führböter (1966):

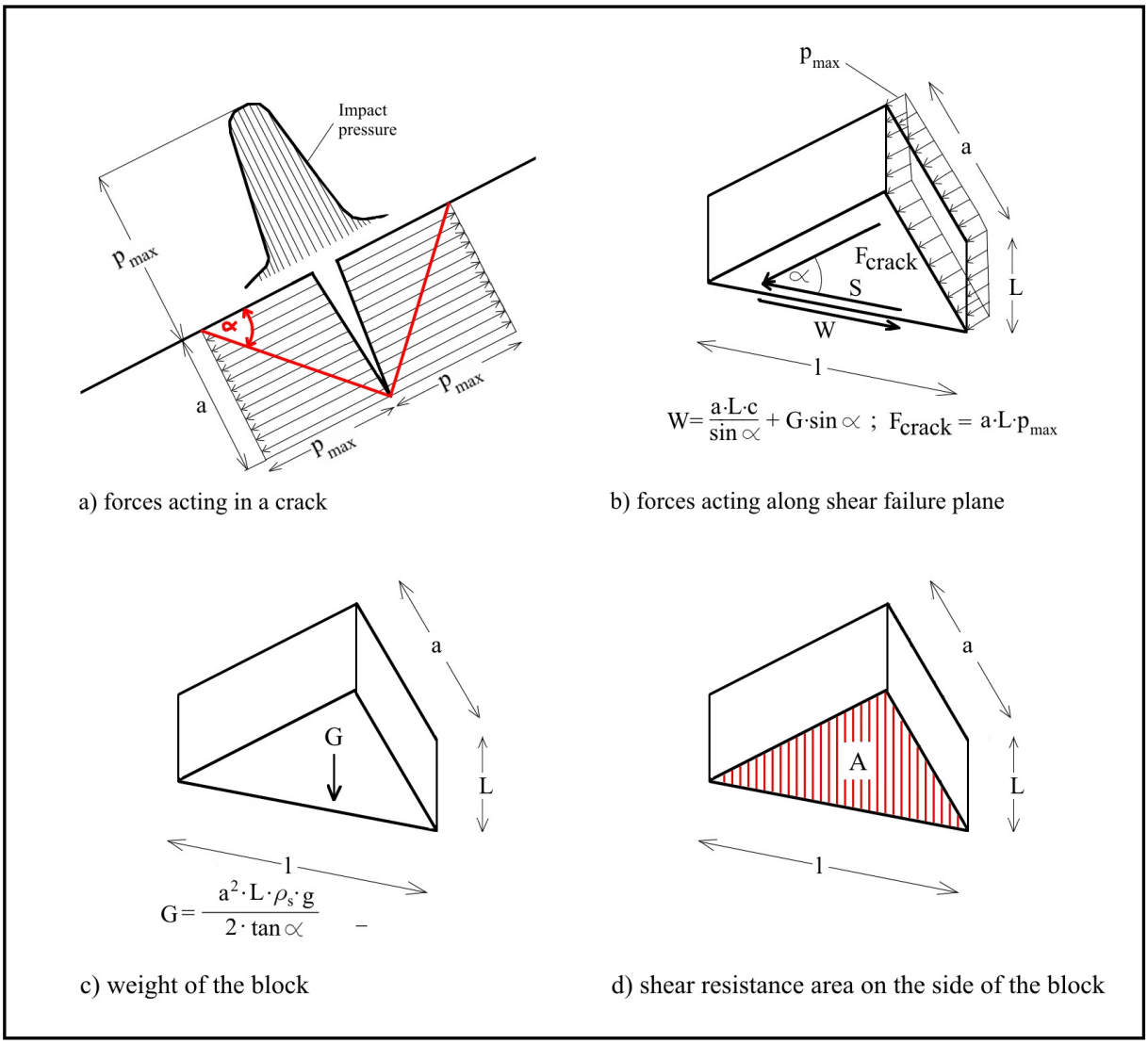

Figure 22: Forces acting on the block of soil

Taking also the weight of the block G into account, the resisting force formulated in Eq.(2.6) is modified:

$$W = \frac{a \cdot L \cdot c}{sin\alpha} + G \cdot sin\alpha \tag{4.1}$$

where:

$G = (0.5 \cdot a^2 \cdot L \cdot \rho \cdot g)/\tan\alpha$

Shear force is here calculated similarly to Eq.(2.3) as

$$S = a \cdot L \cdot p_{max} \cdot cos\alpha \tag{4.2}$$

If also the shear resistance W_A on both sides of the block is considered in the calculations, Eq.(4.1) takes the form:

$$W = \frac{a \cdot L \cdot c}{sin\alpha} + G \cdot sin\alpha + W_A \tag{4.3}$$

where:

$$W_A = A \cdot c = \frac{a^2 \cdot c}{\tan\alpha} \tag{4.4}$$

As W=S at the limit state (failure), the angle of shear failure α is calculated iteratively by the following equations:

- including the weight of the block

$$\frac{a \cdot L \cdot c}{sin\alpha} + 0.5 \cdot a^2 \cdot L \cdot \cot\alpha \cdot \rho \cdot g \cdot sin\alpha = a \cdot L \cdot p_{max} \cdot cos\alpha \tag{4.5}$$

- including additionally the shear resistance on both sides of the block

$$\frac{a \cdot L \cdot c}{sin\alpha} + 0.5 \cdot a^2 \cdot L \cdot \cot\alpha \cdot \rho \cdot g \cdot sin\alpha + \frac{a^2 \cdot c}{\tan\alpha} = a \cdot L \cdot p_{max} \cdot cos\alpha \tag{4.6}$$

A comparison between measured angle of shear failure α_{meas} with the calculated value using Eqs (2.7), (4.5) and (4.6) is given in Tab.12 and Figs 23-24.

Approach	Mean $\alpha_{meas}/\alpha_{calc}$	Std.deviation $\alpha_{meas}/\alpha_{calc}$	CoV
Model of Führböter (1966) - Eq.(2.7)	1.165	0.187	0.16
Modified model of Führböter (1966) - (weight of the block included - Eq.(4.5)	1.113	0.172	0.15
Modified model of Führböter (1966) - (weight and shear resistance on sides of the block included- Eq.(4.6)	0.971	0.135	0.14

Table 12: Comparison of the mean, standard deviation and coefficient of variation of α_{meas} / α_{calc} for three approaches

Taking additional resisting forces into account, the results improved from α_{meas} / α_{calc} =1.165 in the case the initial approach of Führböter (1966) to α_{meas} / α_{calc} =0.971 for the approach that includes also the weight of the block and shear resistance on both sides of the block (difference about 17%). The scatter is also getting significantly smaller. However, in some cases no shear failure was predicted, although it occurred in the test.

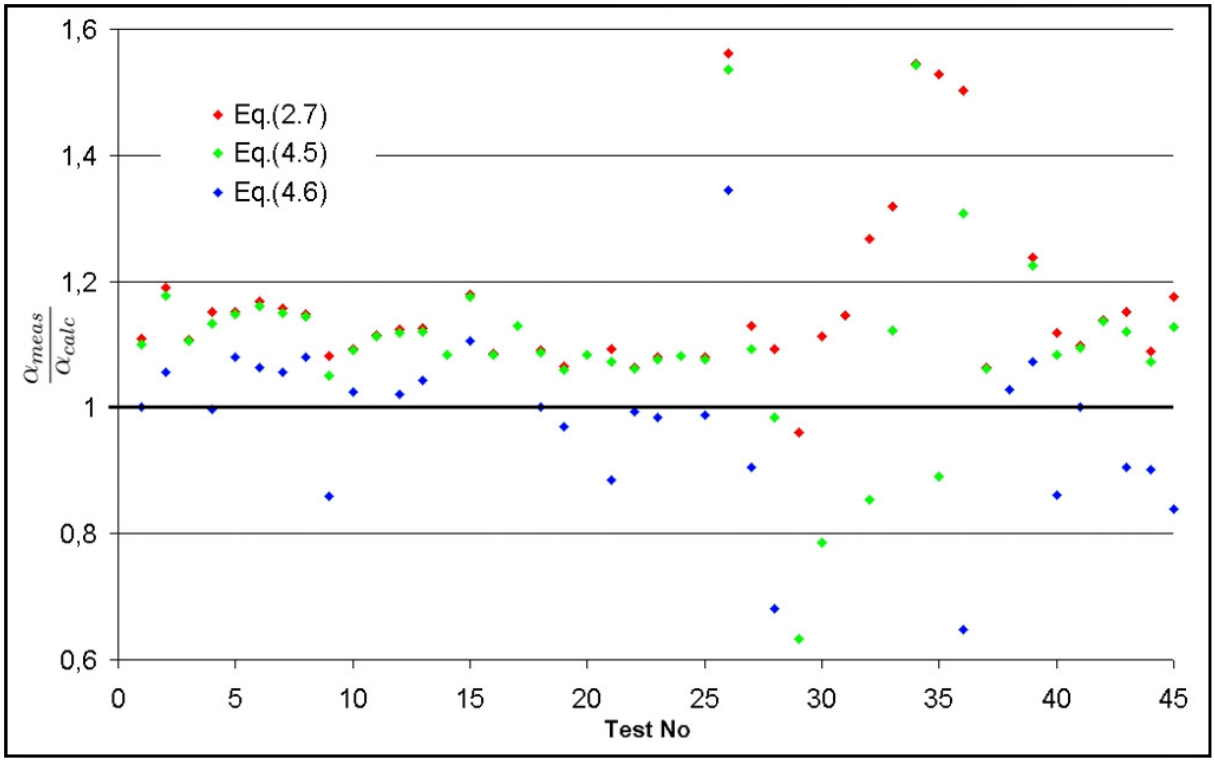

Figure 23: Comparison of different approaches to calculate angle of shear failure

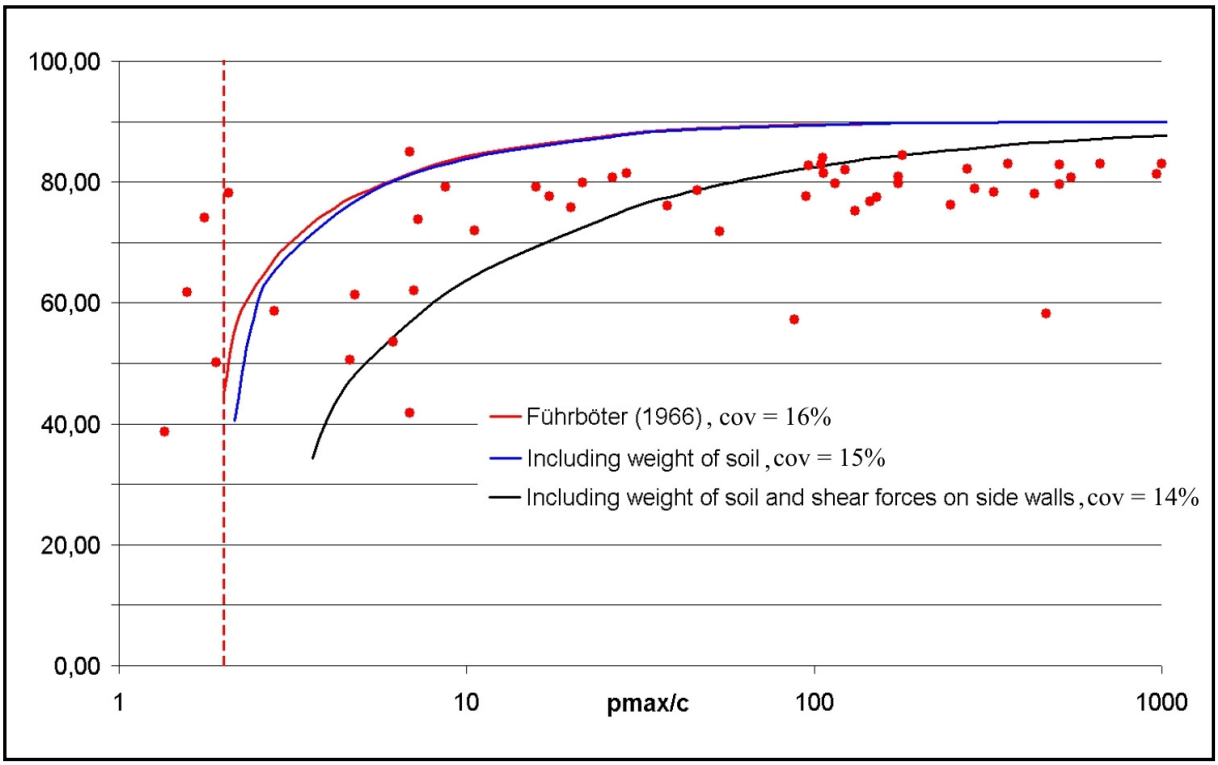

Figure 24: Comparison of different approaches to calculate angle of shear failure

4.2 Grass cover sample with a pre-induced crack

The samples of moderate clay with grass cover taken from a sea-dike (see Section 3.2.2) with an artificially induced crack are used to find out whether the process of shear failure may occur when the crack in a grass cover is subjected to impact pressure. The crack induced for the purposes of this experiment was 100mm deep, 100mm long and 5mm wide (Fig.25).

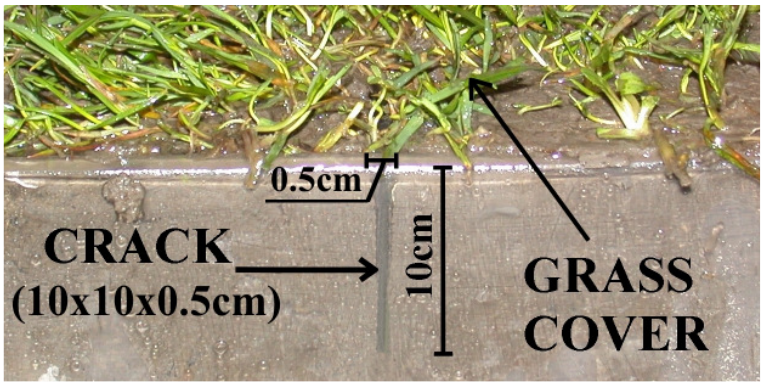

Figure 25: Grass cover with an artificially induced crack

The apparent root cohesion c_r of the grass cover was measured (see Section 3.3.2). Depending on the depth under the surface the values were obtained between c_r = 14 kPa (at the depth of 10cm) and c_r = 94 kPa (at the depth of 2cm), with the mean of c_r = 41 kPa. The measured mean cohesion of the soil is c_s = 7 kPa, which gives the total mean shear strength of the grass cover $c = c_r + c_s$ = 48 kPa. According to the model of Führböter (1966) the impact pressure that is required to induce the shear failure should be of the value $p_{max} = 2 \cdot c = 2 \cdot 48\ kPa = 96\ kPa$.

As the maximal impact pressure that can be generated using the experimental set-up is equal $p_{max} = 24.74\ kPa$, no shear failure is expected to occur. Nevertheless, this was also confirmed experimentally. During the experiment the crack in grass cover was subject to the maximal impact pressure $p_{max} = 24.74\ kPa$. In the first test run no shear failure occurred, so the procedure was repeated five times, as indicated in Section 3.3.4 and in Table 9. The shear failure occurred for none of the tests. For the last test run the crack was subjected to a series of 10 impact pressures. Also in this experiment no shear failure occurred. The intact crack after a series of 10 impact pressure events is shown in the Figure 26.

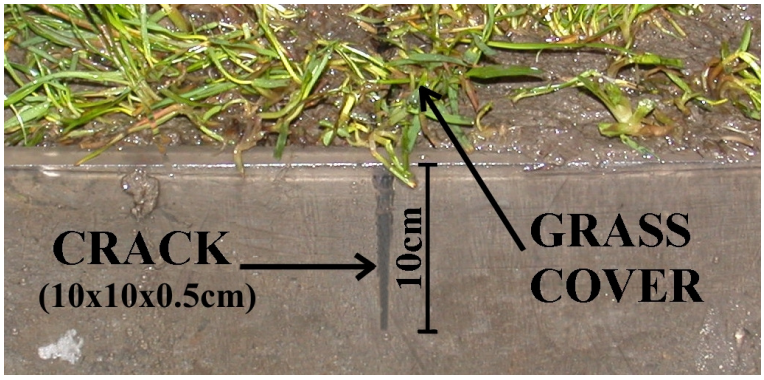

Figure 26: Grass cover with an artificially induced crack after 10 impact pressure events

Since during the experiments with the highest possible impact pressure p_{max} no shear failure occurred, the tests with smaller impact pressures were abandoned. As a conclusion it can be stated, that the shear failure probably would occur if the crack in a sample of grass cover would be subject to a sufficiently large impact pressure, but due to technical reasons it is impossible to induce such an impact pressure using the current experimental set-up shown in Figure 9. It should be also mentioned, that the pull-cracks in grass cover occur very rarely, as the dense network of roots prevents from their occurrence.

4.3 Compacted clay sample with no significant cracks

For every type of clay the experiments are performed as indicated in Section 3.3.5 and Table 10. Applied energies of impact are in range 10-30J. For each given energy the test runs were performed using water layer of given thickness (c.f. Table 10). Tests without a damping water layer were performed as indicated in Section 3.3.5. The results obtained from the tests without a damping water layer are used to calibrate the detachability parameter k_d, which is defined as the mean volume of eroded soil by a unit of energy of a single impact.

The analysis of the results shows that the volume of soil eroded due to a single event doesn't depend linearly on the energy of the impact. For higher energy values, the soil seems to erode more slowly than expected, while for the smaller values it erodes faster than expected. This trend is stronger in the case of the weak clay. In order to account for the nonlinearity of the process a new formula has been introduced:

$$R_{d,p} = p_{max} \cdot k_{d,p} \cdot e^{-w \cdot h} \tag{4.7}$$

where:

- $R_{d,p}$ - volume of the eroded soil $[cm^3]$
- $k_{d,p}$ - detachability parameter $[cm^3/kPa]$
- w - empirical coefficient describing the damping effectivenes of a water layer [-]
- h - thickness of a water layer [cm]

The detachability parameter k_{dp} [cm^3/kPa] is calculated as the mean value of soil volume eroded by a unit impact pressure (1kPa) when no damping water layer is present.

The measured volume of soil k_{dp} [cm^3/kPa] eroded for a unit impact pressure is given in Tabs. A-5, A-7 and A-9 and Figs. 27, 28 and 29 for weak, moderate and strong clay, respectively. The measured volume of eroded soil k_d [cm^3] for a unit energy of the impact (1J) is given in Tab.A-4 for weak, in Tab.A-6 for moderate and in Tab.A-8 for strong clay. According to those results, the coefficients used in Eqs.(2.1) and (4.7) are calibrated as (Tab. 13):

Table 13: The values of coefficients in Eqs.(2.1) and (4.7) calibrated for the used types of soil

Type of the soil	k_d $[cm^3/J]$	$k_{d,p}$ $[cm^3/kPa]$	w [−]	cov
Weak clay	1.17	1.09	0.25	0.16
Moderate clay	1.01	0.99	1.0	0.18
Strong clay	0.88	0.85	0.1	0.55

A clear dependency of the detachability coefficients on the type of the soil can be observed as their values decrease with the increasing quality of the clay. The parameter w doesn't seem to depend on the type of soil for the tested samples.

When the volume of eroded soil is calculated based on the detachability parameter k_d for unit energy, the correlation coefficient R calculated for all the measurements takes the value $R_{kd}=0.570$ for weak clay, $R_{kd}=0.812$ for moderate clay and $R_{kd}=0.310$ for strong clay.

For the calculations based on the dependency of the volume of eroded soil on the k_{dp} parameter for unit impact pressure the correlation coefficient is of the value $R_{kd}=0.742$ for weak clay, $R_{kd}=0.842$ for moderate clay and $R_{kd}=0.336$ for strong clay.

These results would suggest that rather the calculations based on the k_{dp} parameter should be used in further investigations, as the linear dependency of the volume of eroded soil on the impact pressure is observed. Large scatter that is seen on the graphs, especially for the calculations based on k_d is to be explained by stochastic variations in the parameters of soil. This explanation could be confirmed by the symmetrical shape of the scatter. The comparison of eroded volume R_d for a unit impact pressure with the mean value of all measurements performed with given water layer thickness is presented in Fig. 27, Fig.28 and Fig.29 for weak, moderate and strong clay, respectively.

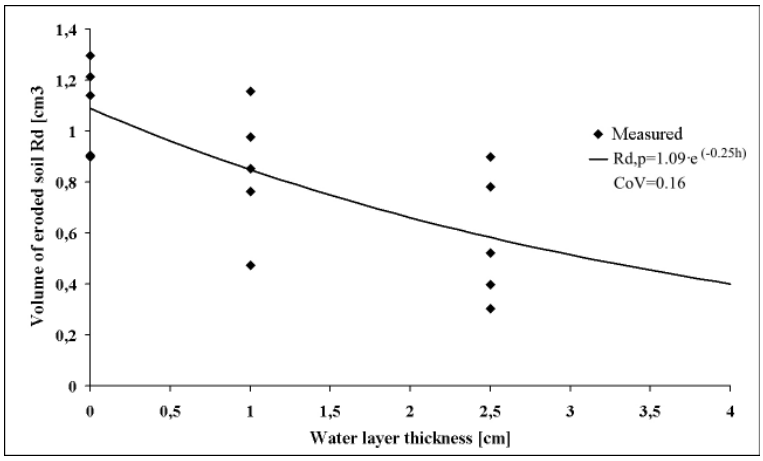

Figure 27: Calculated and measured Volume R_{dp} - weak clay

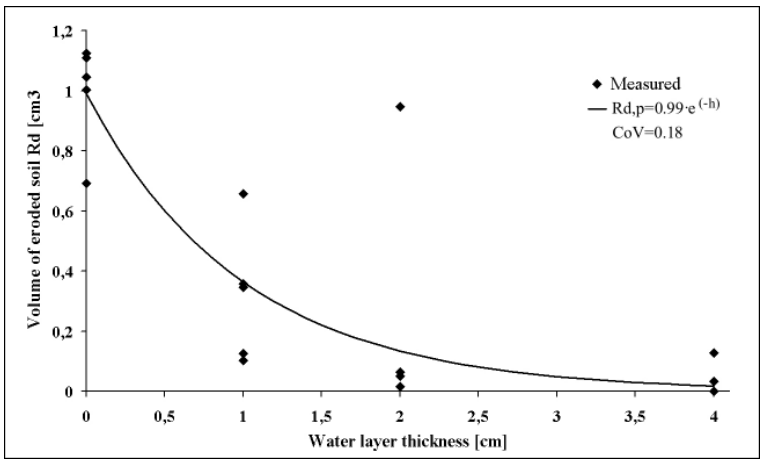

Figure 28: Calculated and measured Volume R_{dp} - moderate clay

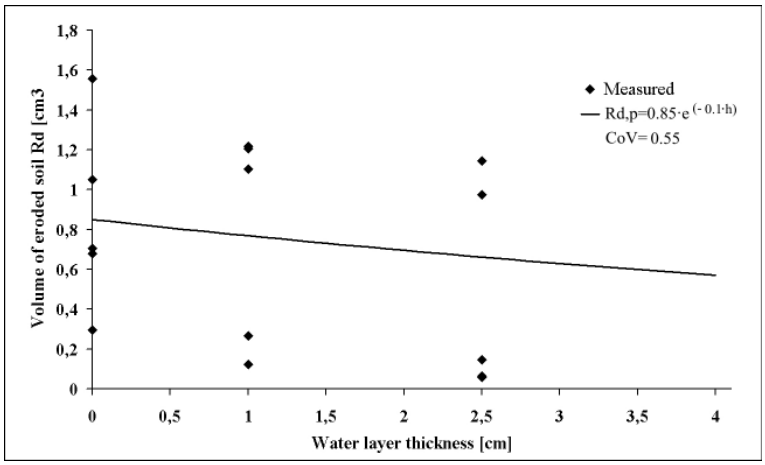

Figure 29: Calculated and measured Volume R_{dp} - strong clay

Good agreement can be observed. For the tests with weak and moderate clay, quite significant influence of the water layer thickness on the progress of erosion can be reported, while for the strong clay the damping effect of the water layer is not so significant. The volume of the soil eroded for a unit energy with 2.5cm of water layer is only about 30% smaller than for the tests with no water layer. For the weak clay there is 44% of the difference, while for the moderate clay even 90%.

In Fig.30 the comparison between the volume of eroded soil measured for all performed experiments and the values calculated using Eq.(2.1) is presented. In Fig.31 the results of comparison between measured values and the ones calculated according to Eq.(4.7) is shown.

Using the dependency of the volume of eroded soil on the pressure gives slightly better results than applying the formula based on the kinetic energy of the impact. The correlation coefficient R for the latter takes the value R_{Rd} =0.63 while for the former R_{Rdp} =0.66. The coefficient of variation is equal to 0.68 and 0.49 for the calculations based on the kinetic energy of the impact and impact pressure, respectively.

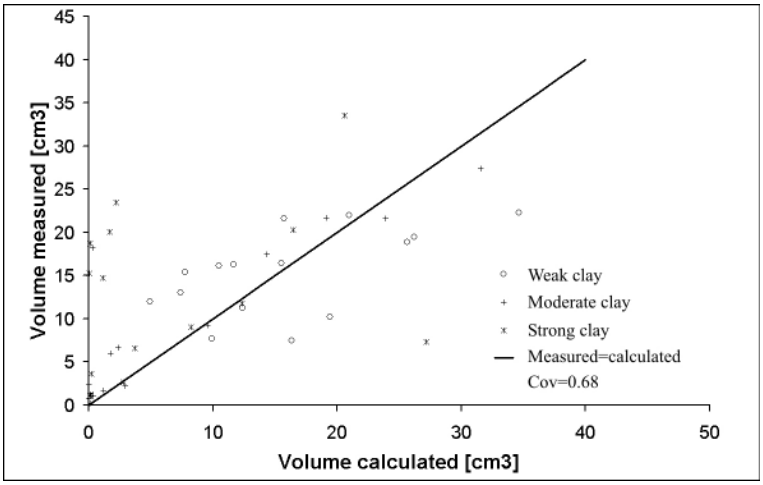

Fig.30: Measured volume of eroded soil vs volume calculated using Eq.(2.1)

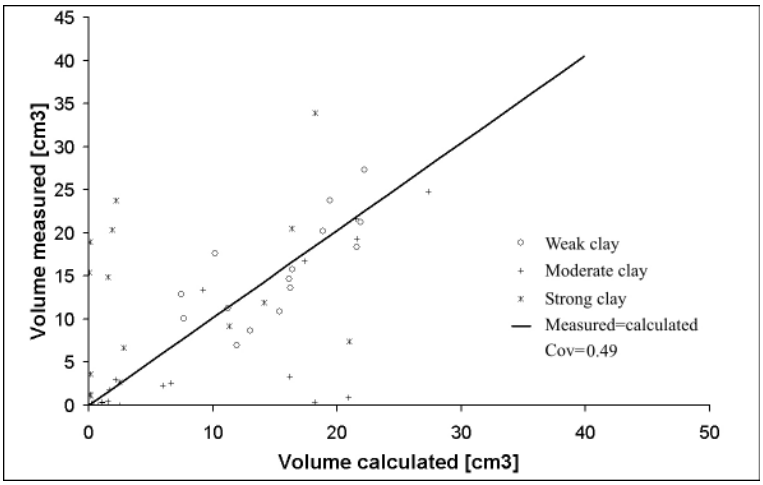

Fig.31: Measured volume of eroded soil vs volume calculated using Eq.(4.7)

During the tests with compacted clay it was observed that for each type of soil a critical impact pressure $p_{max,crit}$ exists. If the acting impact pressure p_{max} is smaller than the critical one $p_{max,crit}$ no erosion occurs. For the weak clay the critical impact pressure $p_{max,crit} \approx 0$ kPa. In the case of moderate clay $p_{max,crit} = 6.3$ kPa, while for the strong clay $p_{max,crit} = 11.7$ kPa. The critical impact pressure for the strong clay is comparable with the pressure induced by the impact of breaking wave of $H_s \approx 0.6$m. It confirms very good the observations made by Delft Hydraulics (1992) that no damage of the clay cover can occur for the waves smaller than $H_s \approx 0.5$m (see Section 2.1.1).

4.4 Grass cover samples - surface erosion

This part of the experimental tests examines the surface erosion of the grass cover subject to a series of impact pressures. The main purpose of these tests is to investigate the influence of the root volume ratio on the progress of erosion. The tests are performed as indicated in Section 3.3.6 and Table 11. In Table A-10 the detachability coefficient k_{dgp} - measured volumes of soil eroded for a unit impact pressure with no water layer are presented. As the soil that formes the substrate of the tested grass cover is classified as weak clay, k_{dp}=1.09 and w=0.25 (see Table 13) will be used in further considerations. The detachability parameter of the grass cover k_{dgp} depends both on the properties of the soil itself and the percentage of the roots that reinforce the soil body (*RVR*). As the root volume ratio decreases with the depth, the detachability parameter increases. The following empirical equation based on the results of the experimental tests gives the dependency of the detachability parameter k_{dgp} on the root volume ratio:

$$k_{d,g,p} = \frac{k_{d,p}}{b \cdot RVR^2} \tag{4.8}$$

where b is the parameter describing the influence of the roots on the erodibility of the grass cover. It takes the value b=5 for the best fit function. In Figure 32 the comparison of the measured values with the ones calculated using Eq.(4.8) is shown. Very good agreement is observed - the correlation coefficient takes the value of R=0.963 and the coefficient of variation is equal .

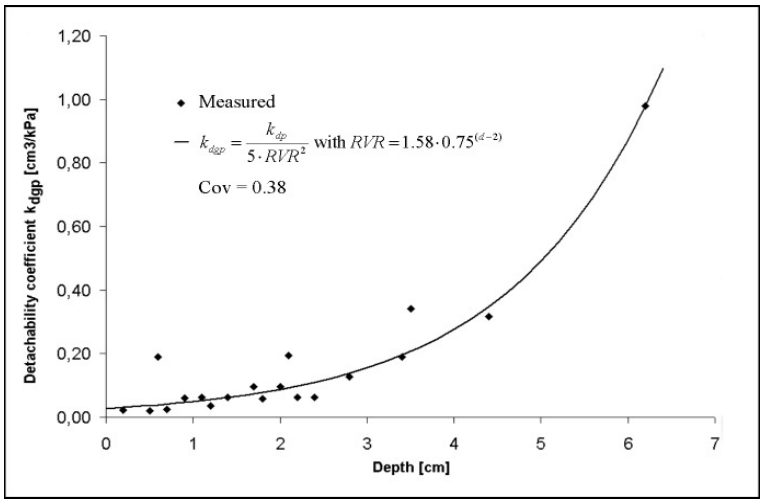

Figure 32: Measured values and best fit function of the detachability parameter $k_{d,g,p}$ with respect to the depth under the surface

At the depth where the RVR=0.5% the detachability parameter of the grass cover k_{dgp} reaches the value of the detachability parameter of the clay k_{dp} - the influence of the roots becomes negligible. This is the ***critical depth of grass erosion*** d_{crit}. Although other parameters as the number of roots per square meter or root tensile strength might also have an influence on the estimation of the critical depth of grass erosion, they are neglected as the Root Volume Ratio is believed to be the most convenient and simple parameter for the estimation of the grass erosion resistance.

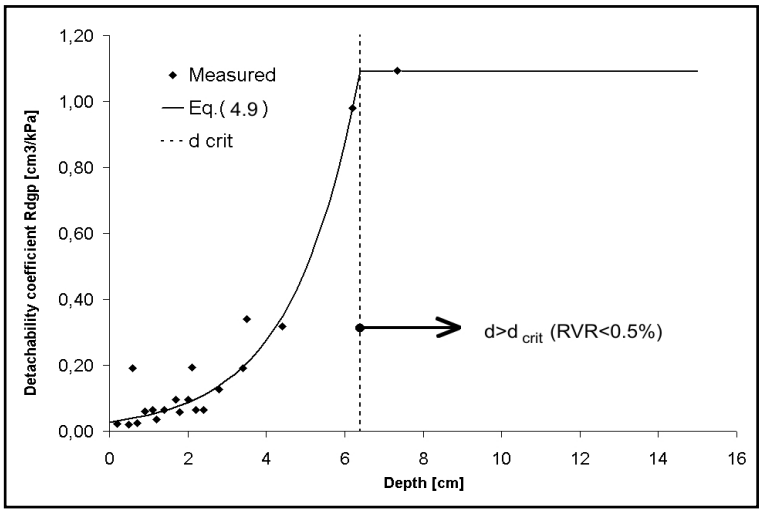

Figure 33: Detachability parameter $k_{d,t,p}$ - values measured and calculated using Eq.(4.9)

The detachability parameter for the whole revetment $k_{d,t,p}$ (Figure 33) is calculated as:

$$k_{d,t,p} = \frac{k_{d,p}}{b \cdot RVR^2} \quad \text{for } d < d_{crit}$$
$$k_{d,t,p} = k_{d,p} \quad \text{for } d > d_{crit} \tag{4.9}$$

The next part of the tests with grass cover subjected to repeated impact pressures should answer the question how the water layer influences the erodibility of the grass cover. In Tables A-11 to A-14 the results of the performed tests are shown. During the tests with a 4cm

thick water layer and impact pressure p_{max}=21.53kPa hardly no erosion occurred - after 270 impact pressure events only about 80cm^3 of the soil eroded. The grass cover is strong enough to withstand quite large impact pressure of p_{max}=21.53kPa (this impact pressure is comparable with a pressure due to impact of breaking wave of the height H=1.1m) that is damped by the thick water layer. Due to this reason, for the tests with an impact pressure p_{max}=19.26kPa and smaller the tests with 4cm thick water layer were not be performed. For the impact pressure p_{max}=19.26kPa almost no erosion occurred also for the water layer of the thickness h=2cm. After 270 impact pressure events less than 70cm^{3}of the grass cover eroded. Because of that for the tests with the impact pressure p_{max}=16.68kPa and smaller also the tests with the water layer of the thickness $h = 2cm$ were abandoned. It was observed, that the damping effect of water layer has a significant influence on the erodibility of the grass cover :

$$R_{d,g,p} = k_{d,g,p} \cdot p_{max} \cdot e^{-w \cdot h} \tag{4.10}$$

where k_{dgp} depends on the depth under the surface and is calculated using Eq.(4.9) while w=0.25. A good agreement can be observed, suggesting that the dependency of the volume of eroded soil on the thickness of water layer is valid not only for the clay, but also for the grass cover. Similarly as in the case of tests with no water layer, also for the tests with a damping water layer of thickness h=1cm, h=2cm and h=4cm a critical depth of erosion has been observed. For all tested configurations the influence of the roots becomes negligible when the root volume ratio becomes smaller than RVR<0.5%. Below this critical depth the detachability parameter of the grass k_{dgp} takes the value of the detachability parameter of the soil k_{dp}. It is therefore confirmed, that the following formula that enables one to calculate the volume of soil eroded for a single impact pressure event including the influence of the water layer:

$$R_{d,t,p} = k_{d,t,p} \cdot p_{max} \cdot e^{-w \cdot h} \tag{4.12}$$

with:

$$\begin{aligned} k_{d,t,p} &= \frac{k_{d,p}}{b \cdot RVR^2} \quad \text{for } d < d_{crit} \\ k_{d,t,p} &= k_{d,p} \quad \text{for } d > d_{crit} \end{aligned} \tag{4.13}$$

is valid for the whole clay cover with vegetation. Figure 34 shows the dependency of the detachability parameter k_{dgp} on the depth under the surface for water layer thickness h=0cm, h=1cm, h=2cm and h=4cm

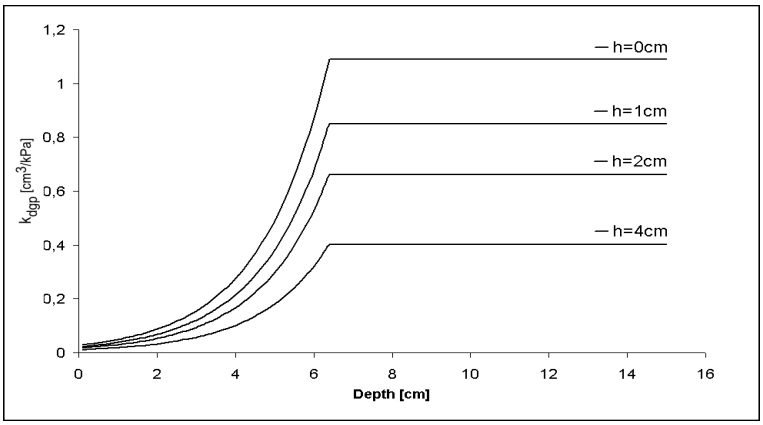

Figure 34: Detachability parameter k_{dgp} - dependency on the water layer thickness and on the depth under the surface

5. Concluding remarks

The effects of the breaking wave impact on the sea-dike cover made of clay and grass are experimentally investigated. Two processes that lead to the failure of revetment were considered:

- the effect of the impact pressures acting on the water-filled cracks and
- the surface erosion of the soil subjected to a series of impact pressure events

The following tentative conclusions may be drawn from the experimental results:

- The conceptual model of Führböter (1966) on the shear failure of the clay cover subjected to the impact pressures acting on a water-filled crack (Section 2.1.2) has been partially confirmed. The shear failure itself indeed occurred. However, the process of the failure significantly differs from the predicted one. Theoretically, a single block of soil should be uplifted due to a shear failure, but during the experimental tests the soil was quarried out from the sample in a form of small lumps and aggregates (Figure 14). Furthermore, as Führböter (1966) neglected additional resisting forces the angle of shear failure α calculated using this approach differed from the measured one. Improvement of the model by taking also additional resisting forces under consideration (Section 4.1.4) provides better results. However, it should be mentioned that the tests with the strong clay seem to be questionable, mostly due to very inhomogeneous structure and technical difficulties with compaction of this type of soil.

- The tests with a crack in a grass cover subject to the impact pressure didn't answer the question whether the shear failure can occur also in this type of dike cover. The maximal impact pressure that can be generated using the available experimental set-up is significantly smaller that the impact pressure that theoretically causes the failure. For none one of the performed tests with grass cover a failure occurred,

- The tests with the clay sample subject to a series of impact pressure events provide results which relatively well fit with the theory of Woolhiser et al. (1990). The coefficients describing the parameters of the soil were calibrated. Also a damping water layer significantly decreases the erodibility of the soil as theoretically predicted,

- As no model of erosion for the grass cover subject to impact pressures is available, empirical formulae based on the results of the performed experiments were developed (Section 4.4). The dependency of the detachability coefficient of the grass cover on the root volume ratio *RVR* (and therefore on the depth under the surface) was demonstrated. The damping effect of the water layer wasinvestigated and shows a relatively good agreement of the measured and calculated values.

Some questions however still remain unanswered. A new experimental device that can generate larger impact pressures has to be developed in order to investigate the shear failure of reinforced soil. Furthermore, the tests on the strong clay should be repeated due to technical problems with soil compaction that occurred during the performed experimental tests. Moreover, grass of different quality and if possible also collected in different season of the year should be investigated.

6. References

1. CAZZUFFI D & CRIPPA E (2005), *Contribution of vegetation to slope stability: an overview of experimental studies carried out on different types of plants*, ASCE, Proceedings of the sessions of the Geo-Frontiers 2005 Congress, Austin,Texas.

2. COPPIN N J & RICHARDS I G (eds) (1990), *Use of vegetation in civil engineering*, CIRIA Book 10,Butterworths,Kent

3. DELFT HYDRAULICS AND SOIL MECHANICS DELFT (1992), *Residual strength of dike coverings, stability of stone settings and clay underlayers: part III, preliminary report on Deltagoot study*. Delft, WL/GD report for RWS-DWW.

4. FÜHRBÖTER A (1966), *Der Druckschlag durch Brecher auf Deichböschungen*, Mitteilungen des Franzius-Instituts für Grund- und Wasserbau der Technischen Universität Hannover, Heft 31

5. FÜHRBÖTER A. & DETTE H H & GRÜNE J (1976), *Response of seadykes due to wave impacts*, Proceedings 15th International Conference Coastal Engineering (ICCE), Honolulu, Hawaii,pp. 2604-2622

6. IGBFM - Institut für Grundbau und Bodenmechanik, Felsmechanik und Tunnelbau (2001), *Belastung der Seedeichbinnenböschungen durch Wellenüberlauf*. Abschlußbericht, University of Essen

7. KORTENHAUS A (2003), *Probabilistische Methoden für Nordseedeiche*, Ph.D-Thesis, Technical University of Braunschweig

8. PACHNIO T (2005), *Laboruntersuchungen zur Druckschlagausbreitung in Fugen, Spalten und Rissen bei Deckwerken*, Diploma Thesis, Technical University of Braunschweig

9. RICHWIEN, W (2003), *Die Widerstandsfähigkeit von Deichen beim Wellenüberlauf und die Entwicklung von Deichbrüchen - eine Bestandsaufnahme*, Essen, 13 p.

10. SHARMA P P & GUPTA S C & RAWLS W J (1991), *Soil detachment by single raindrops of varying kinetic energy*. Soil Science Society of America Journal 55: 301-307.

11. SIMON A & COLLISON A J C (2001), *Quantifying Root Reinforcement of Streambanks for Some Common Riparian Species: Are Willows as Good as It Gets?,*ASCE,Wetlands Engineering and River Restoration Conference 2001,Reno,Nevada.

12. SMITH G M & SEIJFFERT J W W & VAN DER MEER J W (1994), *Erosion and overtopping of a grass dike. Large scale model tests*, Proceedings 24th International Conference Coastal Engineering (ICCE). Kobe, Japan, pp. 2639-2652.

13. SPRANGERS J T C M (1999), *Vegetation dynamics and erosion resistance of seadyke grassland,* Ph.D.-Thesis, Wageningen Agricultural University, Wageningen.

14. TAW (1996), *Clay for dikes. Technical Advisory Committee on Water Retaining Structures, Technical Report*, Delft, The Netherlands, 58

15. TORRI D & SFALANGA M & Del Sette M (1987), *Splash detachment: runoff depth and soil cohesion,* Catena, 14, 149-155.

16. YOUNG M J (2005), *Wave Overtopping and Grass Cover Layer Failure on the Inner Slope of Dikes,* MSc Thesis WSE-CEPD-05.03,UNESCO,Institute for Water Education

17. WEISSMAN R (2003), *Die Wiederstandfähigkeit von Seedeichen gegen ablaufendem Wasser,* PhD-Thesis, University of Duisburg-Essen

18. WOOLHISER D A & SMITH R E & GOODRICH D C (1990), *KINEROS, a Kinematic Runoff and Erosion Model: Documentation and User Manual,* USDA-Agricultural Research Service, ARS-77. US Department of Agriculture: Washington, DC.

APPENDIX

Results of the soil laboratory and impact simulator tests

Table A-1: Comparison of calculated and measured angle of erosion - weak clay

No	Impact pressure $[kPa]$	Water content	Cohesion $[kPa]$	α_{calc} $[deg]$	α_{meas} $[deg]$	$\frac{(\alpha_{meas}-\alpha_{calc})\cdot 100}{\alpha_{meas}}$
1	13.32	0.315	0.08	89.72	80.91	-10.88
2	13.32	0.306	0.10	89.61	75.26	-19.06
3	13.32	0.367	0.01	89.99	81.26	-10.74
4	13.32	0.296	0.14	89.44	77.69	-15.13
5	13.32	0.342	0.03	89.91	78.09	-15.13
6	16.68	0.303	0.12	89.65	76.80	-16.73
7	16.68	0.304	0.11	89.67	77.54	-15.64
8	16.68	0.254	0.58	88.06	81.40	-14.73
9	16.68	0.323	0.06	89.84	82.15	-8.19
10	16.68	0.340	0.05	89.87	78.33	-9.35
11	19.26	0.339	0.04	89.94	80.70	-11.45
12	19.26	0.292	0.17	89.55	79.69	-12.37
13	19.26	0.304	0.11	89.72	79.75	-12.50
14	19.26	0.357	0.02	89.99	83.07	-8.33
15	19.26	0.315	0.08	89.81	76.22	-17.84
16	21.53	0.333	0.04	89.93	82.89	-8.50
17	21.53	0.333	0.04	89.93	79.58	-13.01
18	21.53	0.290	0.18	89.58	82.07	-9.14
19	21.53	0.286	0.20	89.50	84.01	-6.53
20	21.53	0.341	0.03	89.96	83.02	-8.36
21	24.74	0.233	1.14	87.39	79.93	-9.33
22	24.74	0.298	0.14	89.73	84.35	-6.37
23	24.74	0.279	0.26	89.45	82.79	-8.05
24	24.74	0.319	0.07	89.89	83.03	-8.26
25	24.74	0.281	0.24	89.50	82.86	-8.01

Table A-2: Comparison of calculated and measured angle of erosion - moderate clay

No	Impact pressure $[kPa]$	Water content	Cohesion $[kPa]$	α_{calc} $[deg]$	α_{meas} $[deg]$	$\frac{(\alpha_{meas}-\alpha_{calc})\cdot 100}{\alpha_{meas}}$
1	13.32	0.490	0.16	89.35	57.22	-56.14
2	13.32	0.458	0.29	88.76	78.67	-12.83
3	13.32	0.404	0.86	86.38	79.14	-9.14
4	13.32	0.362	1.99	81.52	84.94	4.04
5	13.32	0.365	1.88	82.01	73.73	-11.23
6	16.68	0.307	5.96	67.19	58.63	-14.60
7	16.68	0.334	3.49	77.63	61.32	-26.61
8	16.68	0.354	2.37	81.76	61.99	-31.88
9	16.68	0.563	0.04	89.88	58.18	-54.49
10	16.68	0.332	3.61	77.16	50.53	-52.69
11	19.26	0.339	3.14	80.49	53.58	-50.24
12	19.26	0.623	0.01	89.97	84.71	-6.20
13	19.26	0.345	2.80	81.55	41.72	-95.48
14	19.26	0.839	0.00	89.99	65.90	-36.57
15	19.26	0.448	0.36	88.93	71.83	-23.80
16	21.53	0.386	1.24	86.69	77.58	-11.73
17	21.53	0.711	0.00	89.99	78.74	-14.30
18	21.53	0.477	0.20	89.46	81.46	-9.83
19	21.53	0.527	0.07	89.80	78.95	-13.75
20	21.53	0.393	1.08	87.13	75.75	-15.02
21	24.74	0.400	0.94	87.82	80.71	-8.81
22	24.74	0.354	2.35	84.53	71.90	-17.57
23	24.74	0.418	0.65	88.49	76.05	-16.35
24	24.74	0.344	2.84	83.36	79.16	-5.31
25	24.74	0.273	11.97	52.30	78.19	33.12

Table A-3: Measured angle of shear failure - strong clay

No	Impact pressure $[kPa]$	Water content	Cohesion $[kPa]$	α_{meas} $[deg]$
1	13.32	0.500	17.85	56.22
2	13.32	0.306	183.13	38.28
3	13.32	0.367	88.52	73.37
4	13.32	0.296	206.07	58.84
5	13.32	0.342	118.88	63.68
6	16.68	0.462	28.33	50.32
7	16.68	0.444	34.79	56.48
8	16.68	0.486	21.00	66.99
9	16.68	0.427	43.07	35.04
10	16.68	0.500	17.85	61.72
11	19.26	0.484	21.67	76.04
12	19.26	0.441	36.40	75.83
13	19.26	0.431	40.70	76.49
14	19.26	0.433	39.75	75.11
15	19.26	0.531	12.27	61.74
16	21.53	0.472	24.92	65.12
17	21.53	0.459	29.27	54.59
18	21.53	0.469	25.98	76.46
19	21.53	0.509	15.94	38.69
20	21.53	0.419	47.02	70.36
21	24.74	0.423	44.96	73.50
22	24.74	0.520	14.04	74.06
23	24.74	0.279	254.35	62.46
24	24.74	0.526	13.02	50.07
25	24.74	0.375	80.09	57.45

Table A-4: Volume of eroded soil R_d for a unit energy impact (1 Joule) for weak clay

Energy [J]	Water layer thickness [cm]		
	0	1	2.5
9.62	1.68	1.60	1.24
14.42	1.50	1.13	0.91
19.23	1.14	0.85	0.40
24.03	0.81	0.42	0.46
31.73	0.70	0.59	0.23
Mean	1.17	0.92	0.65

Table A-5: Volume of eroded soil $R_{d,p}$ for 1 kPa of impact pressure - weak clay

Impact pressure [kPa]	Water layer thickness [cm]		
	0	1	2.5
13.32	1.21	1.15	0.89
16.68	1.29	0.97	0.78
19.26	1.14	0.85	0.39
21.53	0.90	0.47	0.52
24.74	0.89	0.76	0.30
Mean	1.09	0.84	0.58

Table A-6: Volume of eroded soil for 1J of energy of impact- moderate clay

Energy [J]	Water layer thickness [cm]			
	0	1	2	4
9.62	0.96	0.17	0.02	0
14.42	1.21	0.41	0.07	0
19.23	1.12	0.27	0.75	0.12
24.03	0.89	0.09	0.04	0.02
31.73	0.86	0.51	0.04	0.0
Mean	1.01	0.29	0.18	0.03

Table A-7: Volume of eroded soil for 1 kPa of impact pressure - moderate clay

Impact pressure [kPa]	Water layer thickness [cm]			
	0	1	2	4
13.32	0.69	0.12	0.01	0
16.68	1.04	0.35	0.06	0
19.26	1.12	0.34	0.94	0.12
21.53	1.00	0.10	0.05	0.03
24.74	1.11	0.65	0.06	0.0
Mean	0.99	0.31	0.22	0.08

Table A-8: Volume of eroded soil R_d for a unit energy of the impact - strong clay

Energy [J]	Water layer thickness [cm]		
	0	1	2.5
9.62	0.94	1.53	1.58
14.42	0.81	1.39	0.07
19.23	1.05	1.2	0.97
24.03	1.39	0.1	0.05
31.73	0.23	0.21	0.11
Mean	0.88	0.88	0.55

Table A-9: Volume of eroded soil for $R_{d,p}$ for a unit impact pressure (1kPa) - strong clay

Impact pressure [kPa]	Water layer thickness [cm]		
	0	1	2.5
13.32	0.68	1.10	1.14
16.68	0.70	1.20	0.06
19.26	1.05	1.21	0.97
21.53	1.55	0.12	0.05
24.74	0.29	0.26	0.14
Mean	0.85	0.78	0.47

Table A-10: The values of the detachability coefficient $k_{d,g,p}$ calibrated for the grass cover

Depth d [cm]	Impact pressure $[kPa]$					
	13.32	16.68	19.26	21.53	24.74	Mean
0.2			0.03	0.02		0.02
0.5			0.03	0.02	0.01	0.02
0.6	0.19					0.19
0.7			0.03	0.02		0.03
0.9	0.06				0.06	0.06
1.1	0.06					0.06
1.2	0.03				0.04	0.04
1.4	0.06					0.06
1.7	0.10					0.10
1.8			0.07		0.04	0.06
2.0	0.10					0.10
2.1		0.19				0.19
2.2	0.06					0.06
2.4	0.06					0.06
2.8	0.13					0.13
3.4	0.19					0.19
3.5		0.34				0.34
4.4	0.32					0.32
6.2		0.98				0.98

Table A-11: The detachability coefficient $k_{d,g,p}$ calibrated for the grass cover with respect to the depth - impact pressure $p_{max} = 24.74kPa$

Water layer thickness $[cm]$					
1		2		4	
Depth [cm]	$k_{d,g,p}$ $[cm^3/kPa]$	Depth [cm]	$k_{d,g,p}$ $[cm^3/kPa]$	Depth [cm]	$k_{d,g,p}$ $[cm^3/kPa]$
0.30	0.024	0.50	0.079	0.40	0.063
0.60	0.032	1.10	0.190	1.00	0.095
1.00	0.127	1.30	0.063	1.30	0.038
1.20	0.021	1.60	0.127	1.50	0.042
1.60	0.063	2.30	0.089	1.70	0.042
2.00	0.127	4.50	0.698	3.30	0.338

Table A-12: The detachability coefficient $k_{d,g,p}$ calibrated for the grass cover with respect to the depth - impact pressure $p_{max} = 21.53kPa$

Water layer thickness $[cm]$					
1		2		4	
Depth [cm]	$k_{d,g,p}$ $[cm^3/kPa]$	Depth [cm]	$k_{d,g,p}$ $[cm^3/kPa]$	Depth [cm]	$k_{d,g,p}$ $[cm^3/kPa]$
0.20	0.036	0.10	0.005	0.20	0.012
0.40	0.036	0.20	0.012	0.30	0.012
0.60	0.036	0.30	0.012	0.60	0.036
1.00	0.012	0.073	0.60	0.044	0.70
1.20	0.029	1.00	0.049	0.80	0.012
1.50	0.109	1.20	0.024	1.00	0.024

Table A-13: The detachability coefficient $k_{d,g,p}$ calibrated for the grass cover with respect to the depth - impact pressure $p_{max} = 19.26kPa$

Water layer thickness $[cm]$			
1		2	
Depth [cm]	$k_{d,g,p}$ $[cm^3/kPa]$	Depth [cm]	$k_{d,g,p}$ $[cm^3/kPa]$
0.10	0.020	0.20	0.007
0.40	0.027	0.30	0.014
0.60	0.027	0.40	0.014
0.80	0.041	0.50	0.007
1.00	0.027	0.70	0.027
1.30	0.041	0.70	0.033

Table A-14: The detachability coefficient $k_{d,g,p}$ calibrated for the grass cover with respect to the depth - impact pressure $p_{max} = 16.68kPa$

Water layer thickness $[cm]$	
1	
Depth [cm]	$k_{d,g,p}$ $[cm^3/kPa]$
0.30	0.007
0.50	0.014
0.90	0.014
1.60	0.007
2.20	0.027
5.50	0.033